INTERNATIONAL JOURNAL OF
NUMERICAL ANALYSIS AND MODELING
Volume 18, Number 2, Pages 203–234

APPROXIMATIONS BY MINI MIXED FINITE ELEMENT FOR THE STOKES-DARCY COUPLED PROBLEM ON CURVED DOMAINS

MARÍA GABRIELA ARMENTANO AND MARÍA LORENA STOCKDALE

Abstract. In this work we solve a Stokes-Darcy coupled problem in a plane curved domain using curved elements. We approximate the velocity-pressure pair by applying the MINI-element method, for the whole coupled problem. We show that, under appropriate assumptions about the curved domain, the proposed method has optimal accuracy, with respect to solution regularity, and has a simple implementation. We also present numerical tests which show the good performance of the proposed method.

Key words. Stokes-Darcy problem, mixed finite elements, curved elements, stability analysis.

1. Introduction

The aim of this paper is to introduce and analyze a finite element scheme for solving the Stokes-Darcy coupled problem on curved domains by using curved elements. These elements are suitable for use along the curved part of the boundary and the curved part of the interface Γ. There are a wide number of papers devoted to the numerical resolution of the Stokes-Darcy coupled problem (see, for example, [4, 24, 25, 29, 30, 32] and the references therein). However, to the authors' knowledge, all analysis for the approach are restricted, in general, to the case of polygonal domains and polygonal interface or by replacing the curved domain Ω with a polygonal domain Ω_h. In [34] the authors consider curved interface and work on the interface with a "coarse scale" allowing for the grids, of the Stokes and Darcy regions, to be non-matching across interfaces. We note that, ignoring the difference between the domain Ω and its polygonal approximation Ω_h or ignoring the difference between the interface Γ_I and its polygonal approximation $\Gamma_{I,h}$, we could introduce an error which can not be compensated by an accurate approximation in the polygonal domain. Taking this observation in mind, different finite element techniques have been developed to deal with curved domains by considering curved finite elements that fit exactly the boundary (see, for example, Bernardi [9], Ciarlet and Raviart [22], Scott [33] and Zlâmal [37]). In this work, we consider curved element like those introduced in [37], which are suitable for the curved part of the interface or the boundary of the whole domain under consideration.

In the recent paper [4] the authors propose an alternative formulation of the coupled problem which allows them, in particular, to use the classical MINI elements obtaining optimal order of approximation. In this paper we generalize the ideas introduced in [4] to solve the Stokes-Darcy coupled problem in curved domains by using curved triangles which fit the curved part of the domain. We prove that, under appropriate assumptions of the curved domain, our finite element formulation satisfies the discrete inf-sup conditions, obtaining as a result optimal accuracy with respect to solution regularity. It is important to point out that our ideas could be extended to other families of elements. We focused on the MINI elements since it

Received by the editors December 28, 2019.
2000 *Mathematics Subject Classification.* 65N12, 65N15, 65N30, 74F10, 74S05.

is one of the simplest, lowest order and straightforward implementations that we could consider by using the same continuous finite element for the Stokes and Darcy equations. Numerical experiments are also presented, which confirm the excellent stability and optimal performance of our method.

The rest of the paper is organized as follows. In Section 2 we state the modified coupled Stokes-Darcy problem in a curved domain. Section 3 is devoted to describe the curved elements under consideration. In Section 4 we present the finite element approximation of the modified Stokes-Darcy problem. Finally, in section 5, we present numerical examples.

2. Problem statement

We consider a bounded open domain $\Omega \subset \mathbb{R}^2$ divided into two open subdomains Ω_S and Ω_D, where the indices S and D stand for fluid and porous regions, respectively. We assume that $\overline{\Omega} = \overline{\Omega}_S \cup \overline{\Omega}_D$, $\Omega_S \cap \Omega_D = \emptyset$ and $\overline{\Omega}_S \cap \overline{\Omega}_D = \Gamma_I$ so, Γ_I represents the interface between the fluid and the porous medium. The remaining parts of the boundaries are denoted by $\Gamma_S = \partial\Omega_S \setminus \Gamma_I$ and $\Gamma_D = \partial\Omega_D \setminus \Gamma_I$, as illustrated in Figure 1. We suppose that Γ_I, Γ_S and Γ_D are piecewise smooth Lipschitz boundaries, more precisely, that Γ_I, Γ_S and Γ_D belongs to piecewise C^{k+1} with $k \geq 1$ sufficiently large to fulfill our requirements.

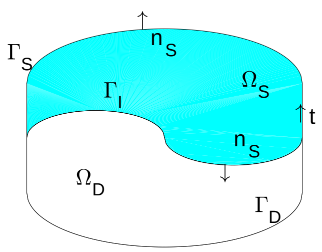

FIGURE 1. Example of two-dimensional curved domain Ω.

We denote by $\boldsymbol{n}_S$ the unit outward normal direction on $\partial\Omega_S$ and by $\boldsymbol{n}_D$ the normal direction on $\partial\Omega_D$, oriented outward. On the interface Γ_I, we have $\boldsymbol{n}_S = -\boldsymbol{n}_D$.

The Stokes-Darcy coupled problem describes the motion of an incompressible viscous fluid occupying a region Ω_S which flows across the common interface through a porous medium living in another region Ω_D saturated with the same fluid. The mathematical model of this problem can be defined by two separate set of equations and a set of coupling terms.

For any function $\mathbf{v}$ defined in Ω, taking into account that its restriction to Ω_S or to Ω_D could play different mathematical roles (especially their traces on Γ_I), we define $\mathbf{v}_S = \mathbf{v}|_{\Omega_S}$ and $\mathbf{v}_D = \mathbf{v}|_{\Omega_D}$.

In Ω_S, the fluid motion is governed by the Stokes equations for the velocity $\mathbf{u}_S$ and the pressure p_S:

$$\left\{\begin{aligned} -\mu\Delta\mathbf{u}_S + \nabla p_S &= \mathbf{f}_S, \text{ in } \Omega_S, \\ \operatorname{div}\, \mathbf{u}_S &= 0, \text{ in } \Omega_S, \\ \mathbf{u}_S &= 0, \text{ in } \Gamma_S, \end{aligned}\right. \tag{1}$$

where $\mathbf{f}_S \in (L^2(\Omega_S))^2$ represents the force per unit mass and $\mu > 0$ the viscosity.

In Ω_D, the porous media flow motion is governed by Darcy's law for the velocity $\mathbf{u}_D$ and the pressure p_D:

$$
(2) \qquad \begin{cases} \dfrac{\mu}{K}\mathbf{u}_D + \nabla p_D = \mathbf{f}_D, \text{ in } \Omega_D, \\ \text{div } \mathbf{u}_D = g_D, \text{ in } \Omega_D, \\ \mathbf{u}_D \cdot \boldsymbol{n}_{\boldsymbol{D}} = 0, \text{ in } \Gamma_D, \end{cases}
$$

where $\mathbf{f}_D \in (L^2(\Omega_D))^2$ represents the force per unit mass, $g_D \in L^2(\Omega_D)$ a source and K denoting the permeability tensor reduced to a positive scalar in the isotropic case considered here.

In Γ_I, we consider the following interface conditions (see, for example, [25]):

$$
(3) \qquad \begin{cases} \mathbf{u}_D \cdot \boldsymbol{n}_D + \mathbf{u}_S \cdot \boldsymbol{n}_S = 0, \\ p_S\, \boldsymbol{n}_S - \mu \nabla \mathbf{u}_S\, \boldsymbol{n}_S - p_D\, \boldsymbol{n}_S - \mu \dfrac{\alpha}{\sqrt{K}} (\mathbf{u}_S \cdot \boldsymbol{t})\, \boldsymbol{t} = 0, \end{cases}
$$

where the first equation represents mass conservation and the second is due to the balance of normal forces and the Beavers-Joseph-Saffman condition, with $\nabla \mathbf{u} = \left(\frac{\partial u_i}{\partial x_j} \right)_{1 \le i,j \le 2}$, α a parameter determined by experimental evidence and $\boldsymbol{t}$ the tangent vector on Γ_I (we recommend [8] for more details on the interface conditions).

We will denote with boldface the spaces consisting of vector valued functions. The norms and seminorms in $\mathbf{H}^m(\mathcal{D})$, with m an integer, are denoted by $\|\cdot\|_{m,\mathcal{D}}$ and $|\cdot|_{m,\mathcal{D}}$ respectively and $(\cdot,\cdot)_{\mathcal{D}}$ denotes the inner product in $L^2(\mathcal{D})$ or $\mathbf{L}^2(\mathcal{D})$ for any subdomain $\mathcal{D} \subset \Omega$. The domain subscript is dropped for the case $\mathcal{D} = \Omega$. Let $\mathbf{H}(\text{div}, \Omega) = \{\mathbf{v} \in \mathbf{L}^2(\Omega) : \text{ div } \mathbf{v} \in L^2(\Omega)\}$, $\mathbf{H}_0(\text{div}, \Omega) = \{\mathbf{v} \in \mathbf{L}^2(\Omega) : \text{ div } \mathbf{v} \in L^2(\Omega), \mathbf{v} \cdot \boldsymbol{n}_D = 0 \text{ on } \Gamma_D\}$ and $L^2_0(\Omega) = \{q \in L^2(\Omega) : \int_\Omega q = 0\}$.

We define the spaces

$$
\mathbf{V} = \{\mathbf{v} \in \mathbf{H}(\text{div}, \Omega) : \mathbf{v}_S \in \mathbf{H}^1(\Omega_S), \mathbf{v} = \mathbf{0} \text{ on } \Gamma_S, \text{ and } \mathbf{v} \cdot \boldsymbol{n}_D = 0 \text{ on } \Gamma_D\}
$$

and

$$
Q = L^2_0(\Omega),
$$

with the norms $\|\mathbf{v}\|_{\mathbf{V}} = (|\mathbf{v}|^2_{1,\Omega_S} + \|\mathbf{v}\|^2_{0,\Omega_D} + \|\text{ div } \mathbf{v}\|^2_{0,\Omega_D})^{\frac{1}{2}} = (|\mathbf{v}|^2_{1,\Omega_S} + \|\mathbf{v}\|^2_{\mathbf{H}(\text{div},\Omega_D)})^{\frac{1}{2}}$ and $\|q\|_Q = \|q\|_0$ respectively.

The mixed variational formulation of the coupled problem (1)-(3) can be stated as follows [4, 29, 30]: Find $(\mathbf{u}, p) \in \mathbf{V} \times Q$ that satisfies

$$
(4) \qquad \begin{cases} a(\mathbf{u}, \mathbf{v}) + b(\mathbf{v}, p) = F(\mathbf{v}) \quad \forall\, \mathbf{v} \in \mathbf{V}, \\ b(\mathbf{u}, q) = G(q) \quad \forall\, q \in Q, \end{cases}
$$

where the bilinear forms $a(\cdot,\cdot)$ and $b(\cdot,\cdot)$ are defined on $\mathbf{V} \times \mathbf{V}$ and $\mathbf{V} \times Q$, respectively, as:

$$
a(\mathbf{u}, \mathbf{v}) = \mu \int_{\Omega_S} \nabla \mathbf{u} : \nabla \mathbf{v} + \mu \frac{\alpha}{\sqrt{K}} \int_{\Gamma_I} (\mathbf{u}_S \cdot \boldsymbol{t})\, (\mathbf{v}_S \cdot \boldsymbol{t}) + \frac{\mu}{K} \int_{\Omega_D} \mathbf{u} \cdot \mathbf{v},
$$

and

$$
b(\mathbf{v}, q) = -\int_\Omega \text{div } \mathbf{v}\, q.
$$

Finally, the linear forms F and G are defined as:

$$
F(\mathbf{v}) = \int_{\Omega_D} \mathbf{f}_D\, \mathbf{v} + \int_{\Omega_S} \mathbf{f}_S\, \mathbf{v} \quad \text{ and } \quad G(q) = -\int_{\Omega_D} g_D\, q.
$$

Then, using the classical theory of mixed methods (see, e.g., Theorem and Corollary 4.1 in Chapter I of [27]) it follows the well-posedness of the continuous formulation (4) and so the following theorem holds.

Theorem 2.1. *There exists a unique* $(\mathbf{u}, p) \in \mathbf{V} \times Q$ *solution to (4). In addition, there exists* C*, depending on the continuous inf-sup condition constant for* b*, the coercivity constant (on the null space of* b*) for* a *and the boundedness constants for* a *and* b*, such that*

$$\|\mathbf{u}\|_{\mathbf{V}} + \|p\|_Q \leq C\{\|\mathbf{f}_S\|_{0,\Omega_S} + \|\mathbf{f}_D\|_{0,\Omega_D} + \|g_D\|_{0,\Omega_D}\}.$$

In our previous work [4], with the purpose in mind of the development of a unified discretization for the coupled problem using the same continuous finite element spaces, we introduce a modification to the Darcy equation and we define a modified coupled Stokes-Darcy problem. The variational form of the modified problem is defined as follows: Find $(\mathbf{u}, p) \in \mathbf{V} \times Q$ satisfying

$$\begin{cases} \tilde{a}(\mathbf{u}, \mathbf{v}) + b(\mathbf{v}, p) = L(\mathbf{v}) & \forall\, \mathbf{v} \in \mathbf{V}, \\ b(\mathbf{u}, q) = G(q) & \forall\, q \in Q, \end{cases} \tag{5}$$

where the bilinear forms $\tilde{a}(\cdot,\cdot)$ and $b(\cdot,\cdot)$ are defined on $\mathbf{V} \times \mathbf{V}$, $\mathbf{V} \times Q$, respectively, as:

$$\tilde{a}(\mathbf{u}, \mathbf{v}) = \mu \int_{\Omega_S} \nabla \mathbf{u} : \nabla \mathbf{v} + \frac{\mu}{K} \int_{\Omega_D} \mathbf{u} \cdot \mathbf{v} + \int_{\Omega_D} \operatorname{div}\, \mathbf{u} \operatorname{div}\, \mathbf{v} + \mu \frac{\alpha}{\sqrt{K}} \int_{\Gamma_I} (\mathbf{u}_S \cdot \boldsymbol{t})\, (\mathbf{v}_S \cdot \boldsymbol{t}),$$

and

$$b(\mathbf{v}, q) = -\int_{\Omega} \operatorname{div}\, \mathbf{v}\, q.$$

Finally, the linear forms L and G are defined as:

$$L(\mathbf{v}) = \int_{\Omega_D} \mathbf{f}_D\, \mathbf{v} + \int_{\Omega_S} \mathbf{f}_S\, \mathbf{v} + \int_{\Omega_D} g_D \operatorname{div}\, \mathbf{v} \quad \text{and} \quad G(q) = -\int_{\Omega_D} g_D\, q.$$

Applying the general abstract setting of mixed formulation (see, e.g., Section 5 in Chapter I of [13]) it follows the well-posedness of the continuous formulation (5). The following result holds.

Theorem 2.2. *There exists a unique* $(\mathbf{u}, p) \in \mathbf{V} \times Q$ *solution to (5). In addition, there exists a positive constant* $\tilde{C}$*, depending on the continuous inf-sup condition constant for* b*, the coercivity constant for* $\tilde{a}$ *and the boundedness constants for* $\tilde{a}$ *and* b*, such that*

$$\|\mathbf{u}\|_{\mathbf{V}} + \|p\|_Q \leq \tilde{C}\{\|\mathbf{f}_S\|_{0,\Omega_S} + \|\mathbf{f}_D\|_{0,\Omega_D} + \|g_D\|_{0,\Omega_D}\}.$$

3. Curved elements

The curved elements under consideration, which we use to represent convincingly the curved boundaries of the domain and the interface, were introduced by Zlamal in [37] and can be seen as a natural generalization of the triangular elements. We consider all triangulations of the given domain Ω into triangles completed along the curved part of the boundaries Γ_I, Γ_S and Γ_D by curved elements.

In order to describe the curved elements under consideration, we denote by Γ a generic curved boundary (Γ could represent the curved part of Γ_I, Γ_S or Γ_D). For our analysis some regularity conditions about the boundaries have to be assumed.

Hypothesis **(Ha)**: We assume that, Γ can be divided into a finite number of arcs such that each has a parametric representation $(\phi(s), \psi(s))$, $a \leq s \leq b$, with functions ϕ and ψ the class C^{k+1} and such that at least one of the derivatives of ϕ and ψ is different from zero in (a, b).

We also assume that the boundary of the curved elements consist of an arc $\widehat{P_1P_3} \subset \Gamma$ and of segments $\overline{P_1P_2}$, $\overline{P_2P_3}$ with P_1 and P_3 in the curved boundary and $P_2 \in \Omega$ (see Figure 2). We denote by T the interior of this curve, and by h_T and θ_T the greatest side and smallest angle of the triangle of vertices P_1, P_2 and P_3. Note that we use the same notation to call the curved elements as for classical triangles.

Let $\hat{T}$ be the classical reference triangle, i.e., the triangle of vertices $(0,0), (1,0)$ and $(0,1)$. Then, for each triangle T in the triangulation we introduce an application F which maps the closed triangle $\overline{\hat{T}}$ to the closed triangle $\overline{T}$. In fact, if we denote by

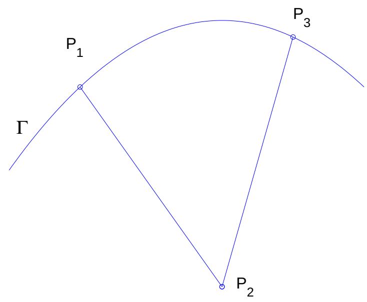

FIGURE 2. Curved triangle.

$(x_j, y_j), 1 \leq j \leq 3$, the coordinates of the vertices P_j of T then, the mapping F it can be defined as (see [37]):

$$F(\xi, \eta) = F_0(\xi, \eta) + (1 - \xi - \eta)(\Phi(\eta), \Psi(\eta)) \tag{6}$$

where F_0 is the affine transformation $\hat{T}$ in the vertices triangle P_1, P_2 and P_3, i.e.,

$$F_0(\xi, \eta) = (x_1 + (x_2 - x_1)\xi + (x_3 - x_1)\eta, y_1 + (y_2 - y_1)\xi + (y_3 - y_1)\eta), \tag{7}$$

and the functions Φ and Ψ are defined as:

$$\Phi(\eta) = \frac{\phi(s_1 + (s_3 - s_1)\eta) - x_1 - (x_3 - x_1)\eta}{1 - \eta} \tag{8}$$

and

$$\Psi(\eta) = \frac{\psi(s_1 + (s_3 - s_1)\eta) - y_1 - (y_3 - y_1)\eta}{1 - \eta} \tag{9}$$

with s_1 and s_3 the values of the parameters corresponding to the vertices P_1 and P_3 respectively. We remark that the point $\eta = 1$ is only an apparent singularity, indeed, it is possible to extend $\Phi(\eta)$ and $\Psi(\eta)$ for $\eta = 1$ such that they belong to C^k for $\eta \in [0, 1]$ (see [37]).

Then, given a polynomial function $\hat{v}(\xi, \eta)$ in $\hat{T}$, with degree p, we can define a function $v(x, y)$ in T as: $v(x, y) = \hat{v}(F^{-1}(x, y))$.

The following lemma, that relates the seminorm of the functions $v(x, y)$ and $\hat{v}(\xi, \eta)$, will be very useful in the demonstrations to be performed, it is a particular case of the Theorem 4.3.2 of [20] or from Lemma 1 of [3].

Lemma 3.1. *If $\hat{v} : \hat{T} \to \mathbb{R}$ is a function on $H^k(\hat{T})$, for $k = 0, 1$, the function $v = \hat{v} \circ F^{-1}$: $T \to \mathbb{R}$ belong to $H^k(T)$ and there is a constant C such that*

$$|v|_{0,T} \leq |J_F|^{\frac{1}{2}}_{\infty,\hat{T}} |\hat{v}|_{0,\hat{T}}, \quad \forall\, \hat{v} \in L^2(\hat{T}) \tag{10}$$

$$|v|_{1,T} \leq C|J_F|^{\frac{1}{2}}_{\infty,\hat{T}} |DF^{-1}|_{\infty,T} |\hat{v}|_{1,\hat{T}}, \quad \forall\, \hat{v} \in H^1(\hat{T}) \tag{11}$$

The next theorem presents some properties of the transformation F, its demonstration is part of Theorem 1 of [37].

Theorem 3.1. *Let Γ be of class C^{k+1} piecewise with $k \geq 1$. If $\tau \geq \tau_0$ with τ_0 a constant > 0 and h is sufficiently small, the transformation F maps $\hat{T}$ one to one on T. The Jacobian $J_F(\xi, \eta)$ of this mapping is different from zero on $\hat{T}$, the side $\overline{R_1 R_3}$ is mapped on* *the arc* $\widehat{P_1P_3}$*, the sides* $\overline{R_1R_2}$ *and* $\overline{R_2R_3}$ *are linearly mapped on the sides* $\overline{P_1P_2}$ *and* $\overline{P_2P_3}$*, respectively. The mapping and its inverse mapping are of class* C^k*. In addition,*

$$c_1h^2 \le |J_F(\xi,\eta)| \le c_2h^2, \quad c_1 = constant > 0, \tag{12}$$

$$D^i x(\xi,\eta) = O(h^{|j|}), \quad D^i y(\xi,\eta) = O(h^{|j|}), \quad 1 \le |i| \le k, \tag{13}$$

$$D^i \xi(x,y) = O(h^{-1}), \quad D^i \eta(x,y) = O(h^{-1}), \quad |i| = 1, \tag{14}$$

where $i = (i_1, i_2), |i| = i_1 + i_2$*,* $D^i u(x,y) = \frac{\partial^{|i|}u}{\partial x^{i_1}\partial y^{i_2}}$ *and* $D^i v(\xi,\eta) = \frac{\partial^{|i|}v}{\partial \xi^{i_1}\partial \eta^{i_2}}$.

4. Finite element approximation of the modified Stokes-Darcy problem

In this section, following the ideas introduced in [4], we apply the MINI-element (in the whole domain) to approximate the velocity-pressure pair, with the particularity that we consider curved elements along the curved part of Γ_I, Γ_S and Γ_D.

Let $\{\mathcal{T}_h\}_{h>0}$ be a family of triangulations of Ω such that any two triangles in $\mathcal{T}_h$ share at most a vertex or an edge and each element $T \in \mathcal{T}_h$ is in either Ω_S or Ω_D. Let $\mathcal{T}_h^S$ and $\mathcal{T}_h^D$ be the corresponding induced triangulations of Ω_S and Ω_D. We assume that the family of triangulations $\{\mathcal{T}_h\}$ satisfies a minimum angle condition, i.e., there exists a constant $\theta_0 > 0$ such that $\theta_T \ge \theta_0$, for any $T \in \mathcal{T}_h$. We also assume that the triangulation $\mathcal{T}_h$ satisfies that: for $T \in \mathcal{T}_h$, we have that T and Γ share at most a vertex or an edge (in particular, T can not have two edges in Γ). We emphasize that now T represents indistinctly a triangle with straight edges or a triangle with a curved edge.

Let $\mathbf{V}_h \subset \mathbf{V}$ and $Q_h \subset Q$ be finite element spaces. The weak formulation (5) leads to the following discrete problem: Find $(\mathbf{v}_h, p_h) \in \mathbf{V}_h \times Q_h$ that satisfies

$$\begin{cases} \tilde{a}(\mathbf{u}_h,\mathbf{v}_h) + b(\mathbf{v}_h,p_h) = L(\mathbf{v}_h) & \forall\, \mathbf{v}_h \in \mathbf{V}_h, \\ b(\mathbf{u}_h,q_h) = G(q_h) & \forall\, q_h \in Q_h. \end{cases} \tag{15}$$

The discretization is said to be uniformly stable if there exist constants $\delta, \gamma > 0$, independent of h, such that

$$\begin{aligned} \tilde{a}(\mathbf{v}_h,\mathbf{v}_h) &\ge \delta \|\mathbf{v}_h\|_{\mathbf{V}}^2 \quad \forall\, \mathbf{v}_h \in \mathbf{V}_h, \\ \sup_{\mathbf{0}\neq \mathbf{v}_h \in \mathbf{V}_h} \frac{b(\mathbf{v}_h,q_h)}{||\mathbf{v}_h||_{\mathbf{V}}} &\ge \gamma ||q_h||_Q \quad \forall\, q_h \in Q_h. \end{aligned} \tag{16}$$

From now on, C represents a positive generic constant, not necessarily the same in each occurrence, which can depend on the mesh only through the parameter θ_0.

For any subdomain $\mathcal{D} \subseteq \Omega$, $k \in \mathbb{N}$, we denote by $W_k(\mathcal{D}) = \{v \in C^0(\mathcal{D}) : v|_T = \hat{v}|_{\hat{T}}(F^{-1}(x,y))$ with $\hat{v}|_{\hat{T}} \in \mathcal{P}_k(\hat{T})\ \forall\, T \in \mathcal{T}_h \cap \mathcal{D}\}$. Note that, due to the presence of curved triangles, the transformation F may not be an affine transformation and therefore the functions in $W_k(\mathcal{D})$ are not necessarily polynomial.

To define then the bases of the spaces involved and the functions relevant to our analysis, we will use definitions in reference elements (similar arguments to the ones we will show here are used in the work [3]).

We introduce the following notation

$$\mathcal{E} = \{\text{all edges in } \mathcal{T}_h\}, \qquad \mathcal{N} = \{\text{all vertices in } \mathcal{T}_h\},$$

and we denote by N the number of vertices in $\mathcal{N}$.

Let A be a set, we define

$$\mathcal{E}_A = \{\ell \in \mathcal{E} : \ell \subset A\}.$$

We decompose

$$\mathcal{E} = \mathcal{E}_{\Omega_S} \cup \mathcal{E}_{\Omega_D} \cup \mathcal{E}_{\Gamma_S} \cup \mathcal{E}_{\Gamma_D} \cup \mathcal{E}_{\Gamma_I}.$$

For $n \in \mathcal{N}$ we denote

$$\omega_n = \bigcup\{T \,|\, T \in \mathcal{T}_h \text{ and } n \in T\}.$$

For any $T \in \mathcal{T}_h$ we define

$$\omega_T = \bigcup \{\omega_n \,|\, n \text{ is a vertex of T }\}.$$

For $\ell \in \mathcal{E}_{\Gamma_I}$ we define

$$\omega_\ell = T_S \cup T_D,$$

where T_S and T_D denote the two triangles sharing ℓ, with $T_S \in \mathcal{T}_h^S$ and $T_D \in \mathcal{T}_h^D$.

The corresponding bubble function in each triangle is defined as follows: for $T \in \mathcal{T}_h$, let

$$b_T(x,y) = \begin{cases} \hat{b}_{\hat{T}}(F^{-1}(x,y)) & \text{in } T \\ 0 & \text{in } \Omega \setminus T, \end{cases}$$

where $\hat{b}_{\hat{T}}$ is the classic cubic bubble given by $\hat{b}_{\hat{T}} = \hat{\delta}_{(0,0),\hat{T}} \hat{\delta}_{(1,0),\hat{T}} \hat{\delta}_{(0,1),\hat{T}}$, where $\hat{\delta}_{(0,0),\hat{T}}, \hat{\delta}_{(1,0),\hat{T}}$ and $\hat{\delta}_{(0,1),\hat{T}}$ denote the barycentric coordinates of $\hat{T}$. As the transformation F send boundaries on boundaries, it is clear that the function b_T it is still a bubble function in T.

Using the properties (12) and (14), it is easy to see that the bubble function satisfies:

$$\int_T b_T \leq C h_T^2 \quad \text{and} \quad \|b_T\|_{1,T} \leq C. \tag{17}$$

We can associate any patch ω_n with a reference patch $\hat{\omega}_n$ as follows (see Figure 3): Let N_n the number of triangles in ω_n, then the corresponding reference patch $\hat{\omega}_n$ is the regular polygon with N_n sides of length 1 that is centered at the origin 0 and is triangulated by N_n triangles that share the vertex 0. The patch ω_n can be related to the reference patch by the following homeomorphism $F_{\omega_n} : \hat{\omega}_n \to \omega_n$ with $F_{\omega_n}(0) = n$ which has the form

$$F_{\omega_n}|_T := F \circ F_A^{-1} \tag{18}$$

where the mapping F_A is the affine transformation between $\hat{T}$ and the triangles in $\hat{\omega}_n$.

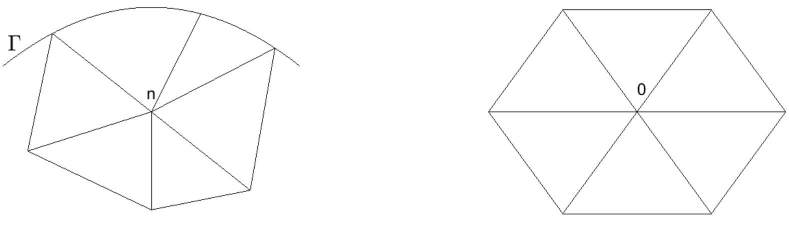

FIGURE 3. ω_n and $\hat{\omega}_n$.

On the other hand, we can associate any patch ω_ℓ with a reference patch $\hat{\omega}_\ell$ (see Figure 4). Moreover, if we enumerate the vertices of T_S and T_D so that the vertices of ℓ are numbered first, i.e., e_1 and e_2 the vertices of ℓ we denote by e_3^S and e_3^D the vertices in Ω_S and Ω_D respectively. Then, associated with ω_ℓ we can define a transformation $F_{\omega_\ell} : \hat{\omega}_\ell \to \omega_\ell$, where $\hat{\omega}_\ell = \hat{T}_1 \cup \hat{T}_2$ with $\hat{T}_1 = \hat{T}$ and $\hat{T}_2$ the triangle of vertices $(0,0), (1,0)$ and $(0,-1)$. The homeomorphism $F_{\omega_\ell} : \hat{\omega}_\ell \to \omega_\ell$ has the form

$$F_{\omega_\ell}|_T := F \circ F_A^{-1} \tag{19}$$

where the mapping F_A is the affine transformation between $\hat{T}$ and the triangles in $\hat{\omega}_\ell$.

In addition, we can define a side bubble function, b_ℓ, as:

$$b_\ell(x,y) = \begin{cases} \hat{b}_{\hat{\ell}}(F_{\omega_\ell}^{-1}(x,y)) & \text{in } \omega_\ell, \\ 0 & \text{in } \Omega \setminus \omega_\ell, \end{cases}$$

where $\hat{\mathrm{b}}_{\hat{\ell}}$ is the piecewise quadratic bubble function defined by $\hat{\mathrm{b}}_{\hat{\ell}}|_{\hat{T}_i} = \hat{\delta}_{(0,0),\hat{T}_i} \hat{\delta}_{(1,0),\hat{T}_i}$, $i = 1, 2$.

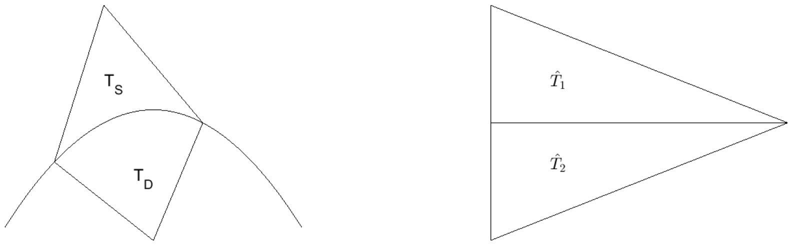

FIGURE 4. ω_ℓ and $\hat{\omega}_\ell$.

Associated with each side $\ell \in \Gamma_I$ we define the bubble functions $v_{\ell,1}$ y $v_{\ell,2}$ with support in ω_ℓ as follows. Let $\hat{T}_1 = \hat{T}$ the classic triangle of reference, i.e., the triangle of vertices $(0,0),(1,0)$ y $(0,1)$ and $\hat{T}_2$ the triangle of vertices $(0,0),(1,0)$ and $(0,-1)$. For each triangle $T_k \subset \omega_\ell\,(k = S$ or $D)$, we denote by e_1, e_2 and e_3 the vertices of T_k, such that e_1 and e_2 are vertices of ℓ and e_3 is the vertex of T_k that is not over Γ_I. If we denote by (x_j, y_j), $1 \leq j \leq 3$, the coordinates of vertices e_j of $T_k\,(k = S$ or $D)$, then the transformation of $\hat{T}_i\,(i = 1$ or $2)$ in the triangle of vertices e_1, e_2 and e_3 it can be defined as in (19).

For example in $\hat{T}_1$ we consider the Lagrangian bases $\hat{\beta}_{1,\hat{T}_1}$ and $\hat{\beta}_{2,\hat{T}_1}$ such that: $\hat{\beta}_{1,\hat{T}_1}(\frac{1}{4},0) = 1$, $\hat{\beta}_{1,\hat{T}_1}(\frac{3}{4},0) = 0$ and $\hat{\beta}_{1,\hat{T}_1}(0,1) = 0$, and $\hat{\beta}_{2,\hat{T}_1}(\frac{1}{4},0) = 0$, $\hat{\beta}_{2,\hat{T}_1}(\frac{3}{4},0) = 1$ and $\hat{\beta}_{2,\hat{T}_1}(0,1) = 0$. Therefore, the corresponding base functions in T_S turn out to be $\beta_{T_S,i} = \hat{\beta}_{i,\hat{T}_1} \circ F^{-1}_{\omega_\ell}(x,y)$, $i = 1,2$. Applying the same reasoning in $\hat{T}_2$ we obtain that the corresponding base functions in T_D are $\beta_{T_D,i} = \hat{\beta}_{i,\hat{T}_2} \circ F^{-1}_{\omega_\ell}(x,y)$, $i = 1,2$, where $\hat{\beta}_{1,\hat{T}_2}$ and $\hat{\beta}_{2,\hat{T}_2}$ are such that: $\hat{\beta}_{1,\hat{T}_2}(\frac{1}{4},0) = 1$, $\hat{\beta}_{1,\hat{T}_2}(\frac{3}{4},0) = 0$ and $\hat{\beta}_{1,\hat{T}_2}(0,-1) = 0$, and $\hat{\beta}_{2,\hat{T}_2}(\frac{1}{4},0) = 0$, $\hat{\beta}_{2,\hat{T}_2}(\frac{3}{4},0) = 1$ and $\hat{\beta}_{1,\hat{T}_2}(0,-1) = 0$.

Then, we define the bubbles $v_{\ell,1}$ and $v_{\ell,2}$ such that, $v_{\ell,i}|_{T_S} = (\hat{\delta}_{(0,0),\hat{T}_1}\hat{\delta}_{(1,0),\hat{T}_1}\hat{\beta}_{i,\hat{T}_1})$ $\circ F^{-1}_{\omega_\ell}(x,y)$ y $v_{\ell,i}|_{T_D} = (\hat{\delta}_{(0,0),\hat{T}_2}\hat{\delta}_{(1,0),\hat{T}_2}\hat{\beta}_{i,\hat{T}_2}) \circ F^{-1}_{\omega_\ell}(x,y)$, $i = 1,2$ (see Figure 5).

The finite element spaces for velocities and pressures are

$$
\begin{aligned}
\mathbf{V}_h := \{\ & \mathbf{v}_h \in \mathbf{L}^2(\Omega), \mathbf{v}_h|_{\Omega_S} \in (C^0(\Omega_S))^2, \mathbf{v}_h|_{\Omega_S} \in (C^0(\Omega_D))^2 : \\
& \mathbf{v}_h|_T = \hat{\mathbf{v}}_h|_{\hat{T}}(F^{-1}(x,y)), \hat{\mathbf{v}}_h|_{\hat{T}} \in (P_1(\hat{T}) \oplus < \hat{b}_{\hat{T}} >)^2, \\
& \forall\, T \in \mathcal{T}_h : \mathcal{E}_T \cap \mathcal{E}_{\Gamma_I} = \emptyset, \text{and } \mathbf{v}_h|_T = \hat{\mathbf{v}}_h|_{\hat{T}_i}(F^{-1}_{\omega_\ell}(x,y)), \\
& \hat{\mathbf{v}}_h|_{\hat{T}_i} \in (P_1(\hat{T}_i) \oplus < \hat{b}_{\hat{T}_i} >)^2 \\
& \oplus < \hat{\delta}_{(0,0),\hat{T}_i}\hat{\delta}_{(1,0),\hat{T}_i}\hat{\beta}_{1,\hat{T}_i}, \hat{\delta}_{(0,0),\hat{T}_i}\hat{\delta}_{(1,0),\hat{T}_i}\hat{\beta}_{2,\hat{T}_i} > (\boldsymbol{n}_\ell \circ F_{\omega_\ell}), \\
& \forall\, T \in \mathcal{T}_h : \mathcal{E}_T \cap \mathcal{E}_{\Gamma_I} = \ell \text{ where } i = 1 \text{ if } T = T_S \text{ or } i = 2 \text{ if not}, \\
& \mathbf{v}_h = 0 \text{ on } \Gamma_S, \mathbf{v}_h \cdot \boldsymbol{n}_D = 0 \text{ on } \Gamma_D \text{ and } \mathbf{v}_h^D \cdot \boldsymbol{n}_D + \mathbf{v}_h^S \cdot \boldsymbol{n}_S = 0 \text{ on } \Gamma_I \}
\end{aligned}
$$

and

$$
\begin{aligned}
Q_h := & \{q_h|_{\Omega_S} \in C^0(\Omega_S), q_h|_{\Omega_S} \in C^0(\Omega_D) : \\
& q_h|_T = \hat{q}_h|_{\hat{T}}(F^{-1}(x,y)),\ \hat{q}_h|_{\hat{T}} \in P_1(\hat{T})\ \forall\, T \in \mathcal{T}_h\} \cap L^2_0(\Omega).
\end{aligned}
$$

The space corresponding to the velocities $\mathbf{V}_h$ is formed by functions of the form

$$
\mathbf{v} = \mathbf{v}^0 + \sum_{T \in \mathcal{T}_h} \mathbf{c}_T\, b_T + \sum_{\ell \in \mathcal{E}_{\Gamma_I}} (\alpha_{\ell,1} v_{\ell,1} \boldsymbol{n}_\ell + \alpha_{\ell,2} v_{\ell,2} \boldsymbol{n}_\ell),
$$

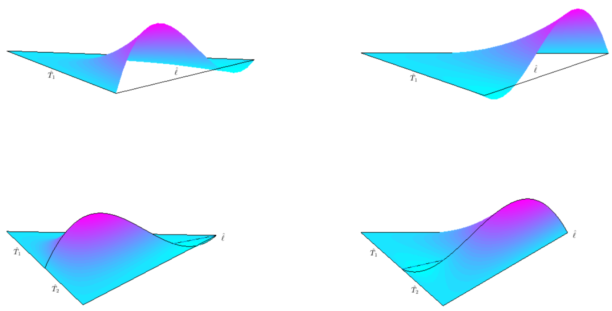

FIGURE 5. The bubble functions $\hat{\delta}_{(0,0),\hat{T}_1}\hat{\delta}_{(1,0),\hat{T}_1}\hat{\beta}_{1,\hat{T}_1}$ and $\hat{\delta}_{(0,0),\hat{T}_1}\hat{\delta}_{(1,0),\hat{T}_1}\hat{\beta}_{2,\hat{T}_1}$ (above) and $\hat{v}_{\ell,1}$ and $\hat{v}_{\ell,2}$ on $\hat{\omega}_\ell$ (bellow).

where $\mathbf{v}^0$ is a continuous function on Ω_D and Ω_S ($\mathbf{v}^0|_T = \hat{\mathbf{v}}^0|_{\hat{T}} \circ F^{-1}(x,y)$ where $\hat{\mathbf{v}}^0|_{\hat{T}}$ is a piecewise linear vector field on $\hat{T}$), b_T it is a bubble function in the triangle T, $\mathbf{c}_T$ it is a constant vector, $v_{\ell,1}$ and $v_{\ell,2}$ are the bubble functions defined above with support in ω_ℓ, and $\alpha_{\ell,i}$, $i = 1, 2$ are constants.

The space corresponding to the pressures Q_h is formed by continuous functions q_h over Ω_D and Ω_S where $q_h|_T = \hat{q}_h|_{\hat{T}} \circ F^{-1}(x,y)$ y $\hat{q}_h|_{\hat{T}}$ is a piecewise linear function on $\hat{T}$.

We use the theory of mixed finite elements to conclude the existence and uniqueness of the solution by finite elements of the discrete problem (15) for these spaces. In order to demonstrate the discrete inf-sup condition (16), we want to construct an operator $\mathbf{\Pi}_h : \mathbf{H}_0^1(\Omega) \longrightarrow \mathbf{V}_h$ such that

1) $b(\mathbf{v} - \mathbf{\Pi}_h\mathbf{v}, q_h) = 0 \quad \forall\, \mathbf{v} \in \mathbf{H}_0^1(\Omega) \quad \forall\, q_h \in Q_h$.
2) $\|\mathbf{\Pi}_h\mathbf{v}\|_{\mathbf{V}} \le C\|\mathbf{v}\|_1$.

We call $W_0(\omega_n) = \{\kappa \in C^0(\omega_n) : \kappa|_{\omega_n} = \hat{\kappa}|_{\hat{\omega}_n} \circ F_{\omega_n}^{-1}(x,y)$ with $\hat{\kappa}|_{\hat{\omega}_n} \in P_0(\hat{\omega}_n)$ and $n \in \Omega_S \cup \Gamma_I^\circ \cup \Omega_D\}$. To define the operator $\mathbf{\Pi}_h$ we use Clement's interpolator.

For any $n \in \mathcal{N}$ and $v \in L^2(\omega_n)$, we can define $\mathcal{P}_{\omega_n} : L^2(\omega_n) \to W_0(\omega_n)$ the orthogonal projection of v in $W_0(\omega_n)$ with respect to the internal product in $L^2(\omega_n)$ that fulfills

$$\int_{\omega_n} v\, p_0 = \int_{\omega_n} \mathcal{P}_{\omega_n}(v)\, p_0 \qquad \forall\, p_0 \in W_0(\omega_n),$$

and then

$$\mathcal{P}_{\omega_n}(v) = \frac{1}{|\omega_n|}\int_{\omega_n} v.$$

To each triangulation $\mathcal{T}_h$ we can associate a "reference triangulation" $\hat{\mathcal{T}}_h$ connecting, for all $n \in \mathcal{N}$, patches ω_n with its corresponding reference patches $\hat{\omega}_n$.

Let $\{\hat{\phi}_i\}_{i\in\{1,\cdots,N\}}$ the Lagrangian base in $\hat{\mathcal{T}}_h$, i.e., given a node $\hat{n}_i$, $\hat{\phi}_i(\hat{n}_i) = 1$ and is zero in the rest of the nodes of the mesh $\hat{\mathcal{T}}_h$.

For any $\mathbf{v} = (v_1, v_2) \in \mathbf{L}^2(\Omega)$ and $n \in \mathcal{N}$ we can define $\mathbf{P}_{\omega_n}(\mathbf{v}) = (\mathcal{P}_{\omega_n}(v_1), \mathcal{P}_{\omega_n}(v_2))$. Then, we consider the following Clement's interpolator:

$$\mathcal{I}\mathbf{v}(x,y) = \sum_{i=1}^{N} \hat{\phi}_i(F^{-1}(x,y))\mathbf{P}_{\omega_{n_i}}(\mathbf{v}).$$

To build the global operator $\mathbf{\Pi}_h$, we impose a condition on each vertex $n \in \mathcal{N}$ according to its location in the domain.

$$\mathbf{\Pi}_h \mathbf{v}(n) = \begin{cases} \mathcal{I}\mathbf{v}(n) = \mathbf{P}_{\omega_n}(\mathbf{v}) & \text{if } n \in \Omega_S, n \in \Omega_D \text{ or } n \in \Gamma_I^\circ \\ \mathbf{0} & \text{in another case,} \end{cases}$$

where Γ° denote, as usual, the interior of Γ_I.

We observe that $\mathbf{\Pi}_h \mathbf{v} = ((\mathbf{\Pi}_h \mathbf{v})_1, (\mathbf{\Pi}_h \mathbf{v})_2)$ then, to simplify notation, we call $\mathbf{\Pi}_{h,j} \mathbf{v} = (\mathbf{\Pi}_h \mathbf{v})_j$ for $1 \leq j \leq 2$.

For each $\ell \in \mathcal{E}_{\Gamma_I}$, we have two degrees of freedom more over ℓ and therefore we can impose that

$$\int_\ell \mathbf{\Pi}_h \mathbf{v} \cdot \boldsymbol{n}_\ell \, \gamma = \int_\ell \mathbf{v}^D \cdot \boldsymbol{n}_\ell \, \gamma, \quad \forall \gamma \in W_1(\Gamma_I),$$

where $\boldsymbol{n}_\ell$ represents the unit normal vector in ℓ with external orientation to Ω_D and $W_1(\Gamma_I) = \{\zeta \in C^0(\Gamma_I) : \zeta|_\ell = \hat{\zeta}|_{\hat{\ell}} \circ F_{\omega_\ell}^{-1}(x, y) \text{ with } \hat{\zeta}|_{\hat{\ell}} \in P_1(\hat{\ell}) \quad \forall \ell \in \mathcal{T}_h \cap \Gamma_I\}$.

The other condition, related to the bubble in each triangle $T \in \mathcal{T}_h$, that we consider to define the operator is the following:

$$\int_T \mathbf{\Pi}_h \mathbf{v} \cdot \, DF^{-1}(j, :) \, dx \, dy = \int_T \mathbf{v} \cdot \, DF^{-1}(j, :) \, dx \, dy \quad j = 1, 2, \tag{20}$$

where DF^{-1} refers to the Jacobian matrix of F^{-1}, i.e., $DF^{-1}(x, y) = \begin{pmatrix} \frac{\partial \xi}{\partial x} & \frac{\partial \xi}{\partial y} \\ \frac{\partial \eta}{\partial x} & \frac{\partial \eta}{\partial y} \end{pmatrix}$.

Now, we write a formula for the global operator on each $T \in \mathcal{T}_h$. Note that there are two cases to consider:

a) $T \in \mathcal{T}_h : \mathcal{E}_T \cap \mathcal{E}_{\Gamma_I} = \emptyset$.
b) $T \in \mathcal{T}_h : \mathcal{E}_T \cap \mathcal{E}_{\Gamma_I} = \ell$.

a) For any triangle $T \in \mathcal{T}_h$ that has no sides in Γ_I, we denote by n_i, $1 \leq i \leq 3$, its vertices and by $\hat{n}_i$ the corresponding ones in $\hat{T}$. Let $\hat{\beta}_i$ be the Lagrange bases in $\hat{T}$, that is, $\hat{\beta}_i(\hat{n}_i) = 1$ and it is zero in the rest of the nodes of $\hat{T}$. In addition, we consider $\beta_i = \hat{\beta}_i|_{\hat{T}} \circ F^{-1}(x, y)$. For each $j = 1, 2$, we observe that the operator restricted to T has the form:

$$\mathbf{\Pi}_{h,j} \mathbf{v}|_T(x, y) \quad = \quad \sum_{i=1}^{3} \alpha_i^j \, \beta_i(x, y) + \gamma^j \, \mathrm{b}_T(x, y),$$

where

$$\alpha_i^j = \begin{cases} \mathcal{P}_{\omega_{n_i}}(v_j) & \text{if } n_i \in \Omega_S, n_i \in \Omega_D \text{ or } n_i \in \Gamma_I^\circ, \\ 0 & \text{if } n_i \in \overline{\Gamma}_S \text{ or } n_i \in \Gamma_D \ , \end{cases}$$

and the constant γ^j is obtained using (20), i.e.,

$$\begin{pmatrix} \int_T \mathrm{b}_T \frac{\partial \xi}{\partial x} \, dx \, dy & \int_T \mathrm{b}_T \frac{\partial \xi}{\partial y} \, dx \, dy \\ \int_T \mathrm{b}_T \frac{\partial \eta}{\partial x} \, dx \, dy & \int_T \mathrm{b}_T \frac{\partial \eta}{\partial y} \, dx \, dy \end{pmatrix} \begin{pmatrix} \gamma^1 \\ \gamma^2 \end{pmatrix}$$

$$= \begin{pmatrix} \int_T (\mathbf{v} - \sum_{i=1}^{3} \beta_i [\alpha_i^1 \; \alpha_i^2]) \, DF^{-1}(1, :) \, dx \, dy \\ \int_T (\mathbf{v} - \sum_{i=1}^{3} \beta_i [\alpha_i^1 \; \alpha_i^2]) \, DF^{-1}(2, :) \, dx \, dy \end{pmatrix}.$$

Let

$$M = \begin{pmatrix} \int_T \mathrm{b}_T \frac{\partial \xi}{\partial x} \, dx \, dy & \int_T \mathrm{b}_T \frac{\partial \xi}{\partial y} \, dx \, dy \\ \int_T \mathrm{b}_T \frac{\partial \eta}{\partial x} \, dx \, dy & \int_T \mathrm{b}_T \frac{\partial \eta}{\partial y} \, dx \, dy \end{pmatrix},$$

note that in the case where the transformation was affine, that is, $F(\xi, \eta) = F_0(\xi, \eta)$, we have $M = (\int_T b_T \, dx \, dy) \, DF^{-1}(x, y) = (\int_T b_T \, dx \, dy) \, DF_0^{-1}(x, y)$, which is obviously invertible.

Without loss of generality, we can assume from now on that:

Assumption **(A1)**: The transformation $F(\xi, \eta)$ is such that $\forall \, T \in \mathcal{T}_h$, M is nonsingular.

Considering the previous hypothesis, we obtain, by a simple calculation, that

$$\gamma^1 = \frac{1}{\Delta}\Bigg[\left(\int_T \mathrm{b}_T \frac{\partial \eta}{\partial y}\,dx\,dy\right)\left(\int_T (\mathbf{v} - \sum_{i=1}^{3} \beta_i[\alpha_i^1\ \alpha_i^2])\,DF^{-1}(1,:)\,dx\,dy\right) - \left(\int_T \mathrm{b}_T \frac{\partial \xi}{\partial y}\,dx\,dy\right)\left(\int_T (\mathbf{v} - \sum_{i=1}^{3} \beta_i[\alpha_i^1\ \alpha_i^2])\,DF^{-1}(2,:)\,dx\,dy\right)\Bigg]$$

and

$$\gamma^2 = \frac{1}{\Delta}\Bigg[-\left(\int_T \mathrm{b}_T \frac{\partial \eta}{\partial x}\,dx\,dy\right)\left(\int_T (\mathbf{v} - \sum_{i=1}^{3} \beta_i[\alpha_i^1\ \alpha_i^2])\,DF^{-1}(1,:)\,dx\,dy\right) + \left(\int_T \mathrm{b}_T \frac{\partial \xi}{\partial x}\,dx\,dy\right)\left(\int_T (\mathbf{v} - \sum_{i=1}^{3} \beta_i[\alpha_i^1\ \alpha_i^2])\,DF^{-1}(2,:)\,dx\,dy\right)\Bigg],$$

where $\Delta = \det\,(M)$, i.e.,

$$\Delta = \left(\int_T \mathrm{b}_T \frac{\partial \xi}{\partial x}\,dx\,dy\right)\left(\int_T \mathrm{b}_T \frac{\partial \eta}{\partial y}\,dx\,dy\right) - \left(\int_T \mathrm{b}_T \frac{\partial \xi}{\partial y}\,dx\,dy\right)\left(\int_T \mathrm{b}_T \frac{\partial \eta}{\partial x}\,dx\,dy\right).$$

We observe that in the case where $F(\xi,\eta) = F_0(\xi,\eta)$ this results in: $\Delta = (\int_T b_T\,dx\,dy)^2 \cdot \det\,(DF_0^{-1}(x,y))$. Using γ^1, γ^2 and Δ, we can write the expression of the operators as follows

$$\begin{aligned}
&\mathbf{\Pi}_{h,1}\mathbf{v}|_T(x,y)\\
&= \sum_{i=1}^{3} \alpha_i^1 \beta_i|_T(x,y)\\
&+ \frac{1}{\Delta}\Bigg[\left(\int_T \mathrm{b}_T \frac{\partial \eta}{\partial y}\,dx\,dy\right)\left(\int_T (\mathbf{v} - \sum_{i=1}^{3} \beta_i[\alpha_i^1\ \alpha_i^2])DF^{-1}(1,:)\,dx\,dy\right)\\
&- \left(\int_T \mathrm{b}_T \frac{\partial \xi}{\partial y}\,dx\,dy\right)\left(\int_T (\mathbf{v} - \sum_{i=1}^{3} \beta_i[\alpha_i^1\ \alpha_i^2])DF^{-1}(2,:)\,dx\,dy\right)\Bigg]\mathrm{b}_T(x,y)
\end{aligned}$$

and

$$\begin{aligned}
&\mathbf{\Pi}_{h,2}\mathbf{v}|_T(x,y)\\
&= \sum_{i=1}^{3} \alpha_i^2 \beta_i|_T(x,y)\\
&+ \frac{1}{\Delta}\Bigg[-\left(\int_T \mathrm{b}_T \frac{\partial \eta}{\partial x}\,dx\,dy\right)\left(\int_T (\mathbf{v} - \sum_{i=1}^{3} \beta_i[\alpha_i^1\ \alpha_i^2])DF^{-1}(1,:)\,dx\,dy\right)\\
&+ \left(\int_T \mathrm{b}_T \frac{\partial \xi}{\partial x}\,dx\,dy\right)\left(\int_T (\mathbf{v} - \sum_{i=1}^{3} \beta_i[\alpha_i^1\ \alpha_i^2])DF^{-1}(2,:)\,dx\,dy\right)\Bigg]\mathrm{b}_T(x,y).
\end{aligned}$$

Now, we modify the projector to consider the different conditions imposed on the vertices when we define the operator

$$\tilde{\mathcal{P}}_{\omega_{n_i}}(v_j) = \begin{cases} \mathcal{P}_{\omega_{n_i}}(v_j) & \text{if } n_i \in \Omega_S,\ n_i \in \Omega_D \text{ or } n_i \in \Gamma_I^{\circ},\\ 0 & \text{if } n_i \in \overline{\Gamma}_S \text{ or } n_i \in \Gamma_D, \end{cases}$$

and therefore $\tilde{\mathbf{P}}_{\omega_{n_i}}(\mathbf{v}) = (\tilde{\mathcal{P}}_{\omega_{n_i}}(v_1), \tilde{\mathcal{P}}_{\omega_{n_i}}(v_2))$.

Then, we use the following modified interpolator

$$\tilde{\mathcal{I}}\mathbf{v}(x,y) = \sum_{i=1}^{N} \hat{\phi}_i(F^{-1}(x,y))\tilde{\mathbf{P}}_{\omega_{n_i}}(\mathbf{v}).$$

Using the above, we can rewrite the operator as follows

$$\begin{aligned}
&\mathbf{\Pi}_{h,1}\mathbf{v}|_T(x,y)\\
=&\tilde{\mathcal{I}}_1\mathbf{v}(x,y)|_T + \frac{1}{\Delta}\Bigg[\left(\int_T \mathrm{b}_T \frac{\partial \eta}{\partial y}\,dx\,dy\right)\left(\int_T (\mathbf{v}-\tilde{\mathcal{I}}\mathbf{v}(x,y))DF^{-1}(1,:)\,dx\,dy\right)\\
&-\left(\int_T \mathrm{b}_T \frac{\partial \xi}{\partial y}\,dx\,dy\right)\left(\int_T (\mathbf{v}-\tilde{\mathcal{I}}\mathbf{v}(x,y))DF^{-1}(2,:)\,dx\,dy\right)\Bigg]\mathrm{b}_T(x,y) \qquad (21)
\end{aligned}$$

and

$$\begin{aligned}
&\mathbf{\Pi}_{h,2}\mathbf{v}|_T(x,y)\\
=&\tilde{\mathcal{I}}_2\mathbf{v}(x,y)|_T\\
&+\frac{1}{\Delta}\Bigg[-\left(\int_T \mathrm{b}_T \frac{\partial \eta}{\partial x}\,dx\,dy\right)\left(\int_T (\mathbf{v}-\tilde{\mathcal{I}}\mathbf{v}(x,y))DF^{-1}(1,:)\,dx\,dy\right)\\
&+\left(\int_T \mathrm{b}_T \frac{\partial \xi}{\partial x}\,dx\,dy\right)\left(\int_T (\mathbf{v}-\tilde{\mathcal{I}}\mathbf{v}(x,y))DF^{-1}(2,:)\,dx\,dy\right)\Bigg]\mathrm{b}_T(x,y). \qquad (22)
\end{aligned}$$

b) Let $T \in \mathcal{T}_h$ be a triangle with one side in Γ_I, that is, $\mathcal{E}_T \cap \mathcal{E}_{\Gamma_I} = \ell$. For each $j = 1, 2$, we observe that the operator restricted to T has the form:

$$\begin{aligned}
\mathbf{\Pi}_{h,j}\mathbf{v}|_T(x,y) \quad = \quad & \sum_{i=1}^{3} \alpha_i^j\, \beta_i|_T(x,y) + \gamma^j\, \mathrm{b}_T(x,y)\\
&+(\alpha_{\ell,1}v_{\ell,1} + \alpha_{\ell,2}v_{\ell,2})|_T(x,y)\, n_{\ell,j}(x,y),
\end{aligned}$$

where

$$\alpha_i^j = \begin{cases} \mathcal{P}_{\omega_{n_i}}(v_j) & \text{if } n_i \in \Omega_S, n_i \in \Omega_D \text{ or } n_i \in \Gamma_I^\circ,\\ 0 & \text{if } n_i \in \overline{\Gamma}_S \text{ or } n_i \in \Gamma_D\ . \end{cases}$$

We define, in the same way as we did previously, the corresponding operator

$$\tilde{\mathcal{P}}_{\omega_{n_i}}(v_j) = \begin{cases} \mathcal{P}_{\omega_{n_i}}(v_j) & \text{if } n_i \in \Omega_S, n_i \in \Omega_D \text{ or } n_i \in \Gamma_I^\circ,\\ 0 & \text{if } n_i \in \overline{\Gamma}_S \text{ or } n_i \in \Gamma_D, \end{cases}$$

and the interpolator

$$\tilde{\mathcal{I}}\mathbf{v}(x,y) = \sum_{i=1}^{N} \hat{\phi}_i(F^{-1}(x,y))\tilde{\mathbf{P}}_{\omega_{n_i}}(\mathbf{v}),$$

with $\tilde{\mathbf{P}}_{\omega_{n_i}}(\mathbf{v}) = (\tilde{\mathcal{P}}_{\omega_{n_i}}(v_1), \tilde{\mathcal{P}}_{\omega_{n_i}}(v_2))$.

To determine γ^j, $\alpha_{\ell,1}$ and $\alpha_{\ell,2}$, in principle, we observe that in this case, we have two degrees of freedom more on ℓ, therefore we can impose that

$$\int_\ell \mathbf{\Pi}_h\mathbf{v}\, \cdot \boldsymbol{n}_\ell\, \gamma = \int_\ell \mathbf{v}^D \cdot \boldsymbol{n}_\ell\, \gamma, \quad \forall\, \gamma \in W_1(\Gamma_I), \qquad (23)$$

where $\boldsymbol{n}_\ell$ represents the unit normal vector in ℓ with outward orientation to Ω_D. Then, γ^j is obtained in such a way that (20) holds.

Therefore, we observe that the operator restricted to T has the form:

$$
\begin{aligned}
\boldsymbol{\Pi}_{h,1}\mathbf{v}|_T(x,y) =& \tilde{\mathcal{I}}_1\mathbf{v}|_T(x,y) \\
&+ \frac{1}{\Delta}\Bigg[\int_T \mathrm{b}_T \frac{\partial \eta}{\partial y}\,dx\,dy\left(\int_T (\mathbf{v}-\tilde{\mathcal{I}}\mathbf{v})DF^{-1}(1,:)\,dx\,dy\right.\\
&\left.-\int_T (\alpha_{\ell,1}v_{\ell,1}+\alpha_{\ell,2}v_{\ell,2})\boldsymbol{n}_\ell DF^{-1}(1,:)\,dx\,dy\right)\\
&-\int_T \mathrm{b}_T \frac{\partial \xi}{\partial y}\,dx\,dy\left(\int_T (\mathbf{v}-\tilde{\mathcal{I}}\mathbf{v})DF^{-1}(2,:)\,dx\,dy\right.\\
&\left.-\int_T (\alpha_{\ell,1}v_{\ell,1}+\alpha_{\ell,2}v_{\ell,2})\boldsymbol{n}_\ell DF^{-1}(2,:)\,dx\,dy\right)\Bigg]\mathrm{b}_T(x,y)\\
&+ (\alpha_{\ell,1}v_{\ell,1}+\alpha_{\ell,2}v_{\ell,2})|_T(x,y)n_{\ell,1}(x,y)
\end{aligned}
\tag{24}
$$

and

$$
\begin{aligned}
\boldsymbol{\Pi}_{h,2}\mathbf{v}|_T(x,y) =& \tilde{\mathcal{I}}_2\mathbf{v}|_T(x,y) \\
&+ \frac{1}{\Delta}\Bigg[-\int_T \mathrm{b}_T \frac{\partial \eta}{\partial x}\,dx\,dy\left(\int_T (\mathbf{v}-\tilde{\mathcal{I}}\mathbf{v})DF^{-1}(1,:)\,dx\,dy\right.\\
&\left.-\int_T (\alpha_{\ell,1}v_{\ell,1}+\alpha_{\ell,2}v_{\ell,2})\boldsymbol{n}_\ell DF^{-1}(1,:)\,dx\,dy\right)\\
&+\int_T \mathrm{b}_T \frac{\partial \xi}{\partial x}\,dx\,dy\left(\int_T (\mathbf{v}-\tilde{\mathcal{I}}\mathbf{v})DF^{-1}(2,:)\,dx\,dy\right.\\
&\left.-\int_T (\alpha_{\ell,1}v_{\ell,1}+\alpha_{\ell,2}v_{\ell,2})\boldsymbol{n}_\ell DF^{-1}(2,:)\,dx\,dy\right)\Bigg]\mathrm{b}_T(x,y)\\
&+ (\alpha_{\ell,1}v_{\ell,1}+\alpha_{\ell,2}v_{\ell,2})|_T(x,y)n_{\ell,2}(x,y),
\end{aligned}
\tag{25}
$$

where, in view of the condition (23), $\alpha_{\ell,1}$ and $\alpha_{\ell,2}$ are such that

$$
\int_\ell (\alpha_{\ell,1}v_{\ell,1}+\alpha_{\ell,2}v_{\ell,2})|_T\,\gamma = \int_\ell (\mathbf{v}^D-\tilde{\mathcal{I}}\mathbf{v})\cdot\boldsymbol{n}_\ell\,\gamma, \quad \forall\,\gamma\in W_1(\Gamma_I),
\tag{26}
$$

with, for $T\subset\omega_\ell$, $v_{\ell,i}|_T = (\hat{\delta}_{(0,0),\hat{T}_j}\,\hat{\delta}_{(1,0),\hat{T}_j}\,\hat{\beta}_{i,\hat{T}_j})\circ F_{\omega_\ell}^{-1}(x,y)$ (where $j=1$ if $T=T_S$ or $j=2$ if not). It is easy to prove that $\alpha_{\ell,1}$ and $\alpha_{\ell,2}$ exist and are unique. First, we note that the number of condition that define $\alpha_{\ell,1}$ and $\alpha_{\ell,2}$ (two because $\gamma\in W_1(\Gamma_I)$) is equal to the degree of freedom (two because we have two unknowns). To demonstrate the existence of $\alpha_{\ell,1}$ and $\alpha_{\ell,2}$, it is enough to prove uniqueness, that is,

$$
\int_\ell (\alpha_{\ell,1}v_{\ell,1}+\alpha_{\ell,2}v_{\ell,2})|_T\,\gamma = 0 \quad \forall\,\gamma\in W_1(\Gamma_I) \quad \text{ if and only if } \quad \alpha_{\ell,1}=\alpha_{\ell,2}=0.
$$

If we consider $\varphi_\ell = [(\alpha_{\ell,1}\hat{\beta}_{1,\hat{T}_j}+\alpha_{\ell,2}\hat{\beta}_{2,\hat{T}_j})\circ F_{\omega_\ell}^{-1}(x,y)]|_\ell$, we have that $\varphi_\ell\in W_1(\Gamma_I)$ and $\int_\ell(\hat{\delta}_{(0,0),\hat{T}_j}\,\hat{\delta}_{(1,0),\hat{T}_j})\circ F_{\omega_\ell}^{-1}\,\varphi_\ell\,\gamma = 0 \quad \forall\,\gamma\in W_1(\Gamma_I)$. Taking, in particular, $\gamma=\varphi_\ell$ we obtain $\int_\ell(\hat{\delta}_{(0,0),\hat{T}_j}\,\hat{\delta}_{(1,0),\hat{T}_j})\circ F_{\omega_\ell}^{-1}\,\varphi_\ell^2 = 0$. We parametrize $\hat{\ell}$ in the following way, $\xi(t)=(t,0)$ with $0\le t\le 1$. Then, as $F_{\omega_\ell}(\xi(t))$ is a parametrization of ℓ we get

$$
\begin{aligned}
0 &= \int_\ell (\hat{\delta}_{(0,0),\hat{T}_j}\, \hat{\delta}_{(1,0),\hat{T}_j}) \circ F_{\omega_\ell}^{-1}\, \varphi_\ell^2 \\
&= \int_0^1 [(\hat{\delta}_{(0,0),\hat{T}_j}\, \hat{\delta}_{(1,0),\hat{T}_j}) \circ \xi(t)][(\alpha_{\ell,1}\hat{\beta}_{1,\hat{T}_j} + \alpha_{\ell,2}\hat{\beta}_{2,\hat{T}_j}) \circ \xi(t)]^2 \\
&\cdot \|(\frac{\partial(F_{\omega_\ell}(\xi(t)))_1}{\partial t}, \frac{\partial(F_{\omega_\ell}(\xi(t)))_2}{\partial t})\|
\end{aligned}
$$

where $(F_{\omega_\ell}(\xi(t)))_i$, $1 \leq i \leq 2$, represents the i-th coordinate of the transformation.

Then, $(\alpha_{\ell,1}\hat{\beta}_{1,\hat{T}_j} + \alpha_{\ell,2}\hat{\beta}_{2,\hat{T}_j}) \circ \xi(t) = 0$ for all t, $0 \leq t \leq 1$, and therefore they must be $\alpha_{\ell,1} = \alpha_{\ell,2} = 0$ as we wanted to see.

We have to verify that the operator $\mathbf{\Pi}_h$ satisfies the following lemma.

Lemma 4.1. *The operator defined above satisfies that*

$$b(\mathbf{v} - \mathbf{\Pi}_h\mathbf{v}, q_h) = 0, \quad \forall\, \mathbf{v} \in \mathbf{H}_0^1(\Omega), \quad \forall\, q_h \in Q_h.$$

Proof. Considering that

$$b(\mathbf{v}, q_h) = -\int_{\Omega_D} \operatorname{div} \mathbf{v}\, q_h - \int_{\Omega_S} \operatorname{div} \mathbf{v}\, q_h,$$

we have that

$$b(\mathbf{v} - \mathbf{\Pi}_h\mathbf{v}, q_h) = -\int_{\Omega_D} \operatorname{div} (\mathbf{v} - \mathbf{\Pi}_h\mathbf{v})\, q_h - \int_{\Omega_S} \operatorname{div} (\mathbf{v} - \mathbf{\Pi}_h\mathbf{v})\, q_h.$$

Summing over all the triangles in both domains, integrating by parts in each triangle we obtain

$$
\begin{aligned}
b(\mathbf{v} - \mathbf{\Pi}_h\mathbf{v}, q_h) &= -\sum_{T\subset\Omega_D} \int_T \operatorname{div} (\mathbf{v} - \mathbf{\Pi}_h\mathbf{v})\, q_h - \sum_{T\subset\Omega_S} \int_T \operatorname{div} (\mathbf{v} - \mathbf{\Pi}_h\mathbf{v})\, q_h \\
&= \sum_{T\subset\Omega_D} \left(\int_T (\mathbf{v} - \mathbf{\Pi}_h\mathbf{v})\, \nabla q_h - \int_{\partial T} q_h(\mathbf{v} - \mathbf{\Pi}_h\mathbf{v}) \cdot \boldsymbol{n}_D \right) \\
&+ \sum_{T\subset\Omega_S} \left(\int_T (\mathbf{v} - \mathbf{\Pi}_h\mathbf{v})\, \nabla q_h - \int_{\partial T} q_h(\mathbf{v} - \mathbf{\Pi}_h\mathbf{v}) \cdot \boldsymbol{n}_S \right).
\end{aligned}
$$

For any $\ell \in \mathcal{E}_{\Omega_S} \cup \mathcal{E}_{\Omega_D}$ we choose a normal unit vector $\mathbf{n}_\ell$ and we denote the two triangles that share that side as T_{in} and T_{out}, with $\boldsymbol{n}_\ell$ pointing to the outside of T_{out}. We define

$$[\mathbf{v} \cdot \boldsymbol{n}_\ell]_\ell := \left(\mathbf{v}|_{T_{\text{out}}}\right) \cdot \boldsymbol{n}_\ell - \left(\mathbf{v}|_{T_{\text{in}}}\right) \cdot \boldsymbol{n}_\ell,$$

which corresponds to the jump of the normal component of $\mathbf{v}$ through the side ℓ. Note that this value is independent of the direction of the normal vector chosen $\boldsymbol{n}_\ell$.

Rewriting the integrals on the edges of the triangles, we obtain

$$
\begin{aligned}
&b(\mathbf{v} - \mathbf{\Pi}_h\mathbf{v}, q_h) \\
=& \sum_{T\subset\Omega_D} \int_T (\mathbf{v} - \mathbf{\Pi}_h\mathbf{v})\, \nabla q_h + \sum_{T\subset\Omega_S} \int_T (\mathbf{v} - \mathbf{\Pi}_h\mathbf{v})\, \nabla q_h \\
&- \frac{1}{2} \sum_{T\subset\Omega_D} \sum_{\ell\in\mathcal{E}_T\cap\Omega_D} \int_\ell [(\mathbf{v} - \mathbf{\Pi}_h\mathbf{v}) \cdot \mathbf{n}_\ell]_\ell\, q_h - \sum_{\ell\in\mathcal{E}_{\Gamma_D}} \int_\ell (\mathbf{v} - \mathbf{\Pi}_h\mathbf{v}) \cdot \boldsymbol{n}_D\, q_h \\
&- \sum_{\ell\in\mathcal{E}_{\Gamma_I}} [\int_\ell (\mathbf{v}^D - \mathbf{\Pi}_h\mathbf{v}) \cdot\, \boldsymbol{n}_D\, q_{D,h} + \int_\ell (\mathbf{v}^S - \mathbf{\Pi}_h\mathbf{v}) \cdot\, \boldsymbol{n}_S\, q_{S,h}] \\
&- \frac{1}{2} \sum_{T\subset\Omega_S} \sum_{\ell\in\mathcal{E}_T\cap\Omega_S} \int_\ell [(\mathbf{v} - \mathbf{\Pi}_h\mathbf{v}) \cdot \mathbf{n}_\ell]_\ell\, q_h - \sum_{\ell\in\mathcal{E}_{\Gamma_S}} \int_\ell (\mathbf{v} - \mathbf{\Pi}_h\mathbf{v}) \cdot \boldsymbol{n}_S\, q_h \\
=& I + II + III + IV + V + VI + VII.
\end{aligned}
$$

The purpose now is to analyze the value of each of the previous terms taking into account the presence of curved triangles.

I - II) We want to see that

$$\int_T (\mathbf{v} - \mathbf{\Pi}_h \mathbf{v}) \cdot \nabla q_{S,h}\, dx\, dy = 0 \quad \forall\, T \subset \Omega_S$$

and

$$\int_T (\mathbf{v} - \mathbf{\Pi}_h \mathbf{v}) \cdot \nabla q_{D,h}\, dx\, dy = 0 \quad \forall\, T \subset \Omega_D.$$

We will prove the first equality, the second is deduced in the same way. As $\hat{q}_{S,h} \in P_1(\hat{T})$, its gradient is constant, therefore we have to

$$\int_T (\mathbf{v} - \mathbf{\Pi}_h \mathbf{v})\, \nabla q_{S,h}\, dx\, dy = \int_T (\mathbf{v} - \mathbf{\Pi}_h \mathbf{v})\, \nabla^{\xi,\eta} \hat{q}_{S,h}\, DF^{-1}(x, y)\, dx\, dy.$$

Now, let's suppose $\nabla^{\xi,\eta} q_{\hat{S},h} = [C_1\ C_2]$ then

$$\begin{aligned}&\int_T (\mathbf{v} - \mathbf{\Pi}_h \mathbf{v})\, \nabla^{\xi,\eta} \hat{q}_{S,h}\, DF^{-1}(x, y)\, dx\, dy \\ &= \int_T (\mathbf{v}_1 - \mathbf{\Pi}_{h,1}\mathbf{v})(C_1 \frac{\partial \xi}{\partial x} + C_2 \frac{\partial \eta}{\partial x}) + (\mathbf{v}_2 - \mathbf{\Pi}_{h,2}\mathbf{v})(C_1 \frac{\partial \xi}{\partial y} + C_2 \frac{\partial \eta}{\partial y})\, dx\, dy.\end{aligned}$$

Rearranging and applying (20) we obtain

$$\begin{aligned}&\int_T C_1[(\mathbf{v}_1 - \mathbf{\Pi}_{h,1}\mathbf{v})\frac{\partial \xi}{\partial x} + (\mathbf{v}_2 - \mathbf{\Pi}_{h,2}\mathbf{v})\frac{\partial \xi}{\partial y}] \\ &+ C_2[(\mathbf{v}_1 - \mathbf{\Pi}_{h,1}\mathbf{v})\frac{\partial \eta}{\partial x} + (\mathbf{v}_2 - \mathbf{\Pi}_{h,2}\mathbf{v})\frac{\partial \eta}{\partial y}]\, dx\, dy \\ =&C_1 \int_T (\mathbf{v} - \mathbf{\Pi}_h \mathbf{v}) DF^{-1}(1, :)\, dx\, dy \\ &+ C_2 \int_T (\mathbf{v} - \mathbf{\Pi}_h \mathbf{v}) DF^{-1}(2, :)\, dx\, dy = 0.\end{aligned}$$

and we conclude that

$$\int_T (\mathbf{v} - \mathbf{\Pi}_h \mathbf{v})\, \nabla q_{S,h}\, dx\, dy = 0.$$

IV - VII) If $\ell \in \mathcal{E}_{\Gamma_S}$, $\mathbf{v} = \mathbf{0} = \mathbf{\Pi}_h \mathbf{v}$ and therefore $\int_\ell (\mathbf{v} - \mathbf{\Pi}_h \mathbf{v}) \cdot \boldsymbol{n}_S\, q_h = 0$. On the other hand, if $\ell \in \mathcal{E}_{\Gamma_D}$, $\mathbf{v} = \mathbf{0} = \mathbf{\Pi}_h \mathbf{v}$ and thus $\int_\ell (\mathbf{v} - \mathbf{\Pi}_h \mathbf{v}) \cdot \boldsymbol{n}_D\, q_h = 0$.

III-VI) For the continuity of the normal component of $\mathbf{v}$ and $\mathbf{\Pi}_h \mathbf{v}$ we have that $\int_\ell [\![(\mathbf{v} - \mathbf{\Pi}_h \mathbf{v}) \cdot \mathbf{n}_\ell]\!]_\ell\, q_h = 0$, for any $\ell \in \mathcal{E}_{\Omega_S} \cup \mathcal{E}_{\Omega_D}$.

V) If $\ell \in \mathcal{E}_{\Gamma_I}$, as $\mathbf{v} \in \mathbf{H}^1_0(\Omega)$ we have that $\int_\ell (\mathbf{v}^S - \mathbf{\Pi}_h \mathbf{v}) \cdot \boldsymbol{n}_S\, q_{S,h} = \int_\ell (\mathbf{\Pi}_h \mathbf{v} - \mathbf{v}^D) \cdot \boldsymbol{n}_D\, q_{S,h}$. Then, to prove that $\int_\ell (\mathbf{v}^D - \mathbf{\Pi}_h \mathbf{v}) \cdot \boldsymbol{n}_D\, q_{D,h} + \int_\ell (\mathbf{v}^S - \mathbf{\Pi}_h \mathbf{v}) \cdot \boldsymbol{n}_S\, q_{S,h} = 0$, it is enough to see that:

$$\int_\ell \mathbf{\Pi}_h \mathbf{v} \cdot \boldsymbol{n}_D\, \delta = \int_\ell \mathbf{v}^D \cdot \boldsymbol{n}_D\, \delta \quad \forall\, \delta \in W_1(\Gamma_I),$$

that is fulfilled by the property (23). Therefore, we can assure that the term V is canceled.

Then, we conclude that the operator $\mathbf{\Pi}_h$ satisfies the first condition of the Fortin operator, that is,

$$b(\mathbf{v} - \mathbf{\Pi}_h \mathbf{v}, q_h) = 0 \quad \forall\, \mathbf{v} \in \mathbf{H}^1_0(\Omega) \quad \forall\, q_h \in Q_h.$$

□

Finally, we need to prove that the operator satisfies the following lemma.

Lemma 4.2. *There exist a constant $C>0$, independent of h, such that*

$$\|\mathbf{\Pi}_h\mathbf{v}\|_{\mathbf{V}} = (|\mathbf{\Pi}_h\mathbf{v}|^2_{1,\Omega_S} + \|\mathbf{\Pi}_h\mathbf{v}\|^2_{\mathbf{H}(div,\Omega_D)})^{\frac{1}{2}} \leq C\|\mathbf{v}\|_1.$$

Proof. First, we analyze $|\mathbf{\Pi}_h\mathbf{v}|_{1,\Omega_S}$.

$$|\mathbf{\Pi}_h\mathbf{v}|^2_{1,\Omega_S} = |\mathbf{\Pi}_{h,1}\mathbf{v}|^2_{1,\Omega_S} + |\mathbf{\Pi}_{h,2}\mathbf{v}|^2_{1,\Omega_S}.$$

We will start by calculating the operator's seminorm $\mathbf{\Pi}_{h,1}\mathbf{v}$ (note that the analysis is similar if instead of $\mathbf{\Pi}_{h,1}\mathbf{v}$ we have $\mathbf{\Pi}_{h,2}\mathbf{v}$)

$$|\mathbf{\Pi}_{h,1}\mathbf{v}|^2_{1,\Omega_S} = \sum_{T\subset\Omega_S:\mathcal{E}_T\cap\mathcal{E}_{\Gamma_I}=\emptyset} |\mathbf{\Pi}_{h,1}\mathbf{v}|^2_{1,T} + \sum_{T\subset\Omega_S:\mathcal{E}_T\cap\mathcal{E}_{\Gamma_I}\neq\emptyset} |\mathbf{\Pi}_{h,1}\mathbf{v}|^2_{1,T}.$$

We will analyze, in principle, the term $I = \sum_{T\subset\Omega_S:\mathcal{E}_T\cap\mathcal{E}_{\Gamma_I}=\emptyset} |\mathbf{\Pi}_{h,1}\mathbf{v}|^2_{1,T}$. From [21] we have that

$$\begin{aligned}
I \leq & C\Big(\sum_{T\subset\Omega_S:\mathcal{E}_T\cap\mathcal{E}_{\Gamma_I}=\emptyset} |\tilde{\mathcal{I}}_1\mathbf{v}(x,y)|^2_{1,T} \\
&+ \sum_{T\subset\Omega_S:\mathcal{E}_T\cap\mathcal{E}_{\Gamma_I}=\emptyset} |\mathrm{b}_T(x,y)|^2_{1,T}\Big(\Big|\Big(\int_T \mathrm{b}_T\frac{\partial\eta}{\partial y}\,dx\,dy\Big)\Big(\int_T(\mathbf{v}-\tilde{\mathcal{I}}\mathbf{v})DF^{-1}(1,:)\,dx\,dy\Big) \\
&- \Big(\int_T \mathrm{b}_T\frac{\partial\xi}{\partial y}\,dx\,dy\Big)\Big(\int_T(\mathbf{v}-\tilde{\mathcal{I}}\mathbf{v})DF^{-1}(2,:)\,dx\,dy\Big)\Big|^2\Big)/|\Delta|^2\Big).
\end{aligned}$$

Applying (17) we obtain

$$\begin{aligned}
I \leq & C\Big(\sum_{T\subset\Omega_S:\mathcal{E}_T\cap\mathcal{E}_{\Gamma_I}=\emptyset} |\tilde{\mathcal{I}}_1\mathbf{v}(x,y)|^2_{1,T} \\
&+ \sum_{T\subset\Omega_S:\mathcal{E}_T\cap\mathcal{E}_{\Gamma_I}=\emptyset} \Big(\Big|\Big(\int_T \mathrm{b}_T\frac{\partial\eta}{\partial y}\,dx\,dy\Big)\Big(\int_T(\mathbf{v}-\tilde{\mathcal{I}}\mathbf{v})DF^{-1}(1,:)\,dx\,dy\Big) \\
&- \Big(\int_T \mathrm{b}_T\frac{\partial\xi}{\partial y}\,dx\,dy\Big)\Big(\int_T(\mathbf{v}-\tilde{\mathcal{I}}\mathbf{v})DF^{-1}(2,:)\,dx\,dy\Big)\Big|^2\Big)/|\Delta|^2\Big).
\end{aligned} \tag{27}$$

Examining the second term we have

$$\begin{aligned}
&\Big|\Big(\int_T \mathrm{b}_T\frac{\partial\eta}{\partial y}\,dx\,dy\Big)\Big(\int_T(\mathbf{v}-\tilde{\mathcal{I}}\mathbf{v})DF^{-1}(1,:)\,dx\,dy\Big) \\
&\quad- \Big(\int_T \mathrm{b}_T\frac{\partial\xi}{\partial y}\,dx\,dy\Big)\Big(\int_T(\mathbf{v}-\tilde{\mathcal{I}}\mathbf{v})DF^{-1}(2,:)\,dx\,dy\Big)\Big|^2 \\
\leq & C\Big[\Big|\int_T \mathrm{b}_T\frac{\partial\eta}{\partial y}\,dx\,dy\Big|^2\Big|\int_T(\mathbf{v}-\tilde{\mathcal{I}}\mathbf{v})DF^{-1}(1,:)\,dx\,dy\Big|^2 \\
&+ \Big|\int_T \mathrm{b}_T\frac{\partial\xi}{\partial y}\,dx\,dy\Big|^2\Big|\int_T(\mathbf{v}-\tilde{\mathcal{I}}\mathbf{v})DF^{-1}(2,:)\,dx\,dy\Big|^2\Big].
\end{aligned}$$

Using the Cauchy-Schwarz inequality, the results (12) and (14), change of variables and that $|T|^{\frac{1}{2}} \sim h_T$ it is easy to see that

$$\Big|\int_T \mathrm{b}_T\frac{\partial\eta}{\partial y}\,dx\,dy\Big|^2 \leq Ch_T^2 \quad \text{and} \quad \Big|\int_T \mathrm{b}_T\frac{\partial\xi}{\partial y}\,dx\,dy\Big|^2 \leq Ch_T^2.$$

Using the same results as before and considering the approximation property given in page 84 of [15] for $\|\hat{v}_1 - \hat{\tilde{\mathcal{I}}}_1\mathbf{v}\|_{0,\hat{T}}$ and $\|\hat{v}_2 - \hat{\tilde{\mathcal{I}}}_2\mathbf{v}\|_{0,\hat{T}}$ we obtain

$$\Big|\int_T(\mathbf{v}-\tilde{\mathcal{I}}\mathbf{v})DF^{-1}(1,:)\,dx\,dy\Big|^2 \leq Ch_T^2\|\mathbf{v}\|_{1,\omega_T}$$

and

$$\Big| \int_T (\mathbf{v} - \tilde{\mathcal{I}}\mathbf{v}) DF^{-1}(2,:)\, dx\, dy \Big|^2 \leq C h_T^2 \|\mathbf{v}\|_{1,\omega_T}.$$

In the previous bound, it was used that: $\|\hat{v}_1\|_{1,\hat{\omega}_T} \leq C\,\|v_1\|_{1,\omega_T} \leq C\,\|\mathbf{v}\|_{1,\omega_T}$, where the first inequality holds by (10).

Then,

$$\begin{aligned}
&\Big|\Big(\int_T \mathrm{b}_T \frac{\partial \eta}{\partial y}\, dx\, dy\Big)\Big(\int_T (\mathbf{v} - \tilde{\mathcal{I}}\mathbf{v}) DF^{-1}(1,:)\, dx\, dy\Big) \\
&\quad - \Big(\int_T \mathrm{b}_T \frac{\partial \xi}{\partial y}\, dx\, dy\Big)\Big(\int_T (\mathbf{v} - \tilde{\mathcal{I}}\mathbf{v}) DF^{-1}(2,:)\, dx\, dy\Big)\Big|^2 \\
&\leq C h_T^4 \|\mathbf{v}\|_1^2.
\end{aligned}$$

Recalling that in the affine $\Delta = (\int_T b_T\, dx\, dy\,)^2 det(DF_0^{-1}(x,y))$ and considering the bounded (17) and (12), it is easy to see that in this case $O(|\Delta|) = h_T^2$.

Assumption **(A2)**: The transformation F is such that, $\forall\, T \in \mathcal{T}_h$, there exist a constant $C > 0$ such that $|\Delta|^2 \geq C\, h_T^4$.

From (27) we obtain

$$I \leq C\Big(\sum_{T \subset \Omega_S : \mathcal{E}_T \cap \mathcal{E}_{\Gamma_I} = \emptyset} |\tilde{\mathcal{I}}_1 \mathbf{v}(x,y)|_{1,T}^2 + \sum_{T \subset \Omega_S : \mathcal{E}_T \cap \mathcal{E}_{\Gamma_I} = \emptyset} \|\mathbf{v}\|_1^2 \Big).$$

For the first term, we observe that fixed i (node of the triangle T), $1 \leq i \leq 3$, the gradient of $\tilde{\mathcal{P}}_{\omega_{n_i}}(v_1)$ is zero, applying the second bounded of (10) we obtain

$$|\tilde{\mathcal{I}}_1 \mathbf{v}|_{1,T} \quad = \quad |\tilde{\mathcal{I}}_1 \mathbf{v} - \tilde{\mathcal{P}}_{\omega_{n_i}}(v_1)|_{1,T} \leq C\, |\hat{\tilde{\mathcal{I}}}_1 \mathbf{v} - \hat{\tilde{\mathcal{P}}}_{\hat{\omega}_{\hat{n}_i}}(v_1)|_{1,\hat{T}}.$$

Applying an inverse estimate (see, for example, Lemma 3.1 of [21]) and the previous approximation property we conclude

$$\begin{aligned}
|\hat{\tilde{\mathcal{I}}}_1 \mathbf{v} - \hat{\tilde{\mathcal{P}}}_{\hat{\omega}_{\hat{n}_i}}(v_1)|_{1,\hat{T}} &\leq C\,\|\hat{\tilde{\mathcal{I}}}_1 \mathbf{v} - \hat{\tilde{\mathcal{P}}}_{\hat{\omega}_{\hat{n}_i}}(v_1)\|_{0,\hat{T}} \\
&\leq C\Big(\|\hat{\tilde{\mathcal{I}}}_1 \mathbf{v} - \hat{v}_1\|_{0,\hat{T}} + \|\hat{v}_1 - \hat{\tilde{\mathcal{P}}}_{\hat{\omega}_{\hat{n}_i}}(v_1)\|_{0,\hat{T}}\Big) \\
&\leq C\,\|\hat{v}_1\|_{1,\hat{\omega}_T} + C\,\|\hat{v}_1 - \hat{\tilde{\mathcal{P}}}_{\hat{\omega}_{\hat{n}_i}}(v_1)\|_{0,\hat{T}}.
\end{aligned}$$

From the approximation property given on page 85 of [15] we obtain that

$$\|\hat{v}_1 - \hat{\tilde{\mathcal{P}}}_{\hat{\omega}_{\hat{n}_i}}(v_1)\|_{0,\hat{T}} \leq C\, h_{\hat{\omega}_{\hat{n}_i}} |\hat{v}_1|_{1,\hat{\omega}_{\hat{n}_i}},$$

then

$$|\tilde{\mathcal{I}}_1 \mathbf{v}|_{1,T} \leq C\,\|\hat{v}_1\|_{1,\hat{\omega}_T} + C\, h_{\hat{\omega}_{\hat{n}_i}} |\hat{v}_1|_{1,\hat{\omega}_{\hat{n}_i}}.$$

As $h_{\hat{\omega}_{\hat{n}_i}} \leq C h_{\hat{T}}$ (see, for example, Lemma 1 of [36])

$$|\tilde{\mathcal{I}}_1 \mathbf{v}|_{1,T} \leq C\,\|\hat{v}_1\|_{1,\hat{\omega}_T}.$$

For the observation we made earlier, $|\tilde{\mathcal{I}}_1 \mathbf{v}|_{1,T} \leq C\,\|\mathbf{v}\|_{1,\omega_T}$.

Since the number of triangles in a neighborhood ω_{n_i} is bounded by a uniform constant,

$$I \leq C\left(\sum_{T \subset \Omega_S : \mathcal{E}_T \cap \mathcal{E}_{\Gamma_I} = \emptyset} \|\mathbf{v}\|_{1,\omega_T}^2 + \sum_{T \subset \Omega_S : \mathcal{E}_T \cap \mathcal{E}_{\Gamma_I} = \emptyset} \|\mathbf{v}\|_1^2 \right) \leq C\,\|\mathbf{v}\|_1^2.$$

We continue now with the analysis of the term $II = \sum_{T \in \Omega_S : \mathcal{E}_T \cap \mathcal{E}_{\Gamma_I} \neq \emptyset} |\mathbf{\Pi}_{h,1}\mathbf{v}|_{1,T}^2$, that is, the case where T has only one side in the interface that we denote by ℓ.

From (24) we have that

$$
\begin{aligned}
II \leq & C\Bigg(\sum_{T\subset\Omega_S:\mathcal{E}_T\cap\mathcal{E}_{\Gamma_I}\neq\emptyset} |\tilde{\mathcal{I}}_1\mathbf{v}(x,y)|^2_{1,T} \\
& + \sum_{T\subset\Omega_S:\mathcal{E}_T\cap\mathcal{E}_{\Gamma_I}\neq\emptyset} \Bigg\{ \Big|\int_T \mathrm{b}_T \frac{\partial\eta}{\partial y}\,dx\,dy\Big|^2 \Bigg[\Big|\int_T (\mathbf{v}-\tilde{\mathcal{I}}\mathbf{v})DF^{-1}(1,:)\,dx\,dy\Big|^2 \\
& + \Big|\int_T (\alpha_{\ell,1}v_{\ell,1}+\alpha_{\ell,2}v_{\ell,2})\boldsymbol{n}_\ell DF^{-1}(1,:)\,dx\,dy\Big|^2\Bigg] \\
& + \Big|\int_T \mathrm{b}_T \frac{\partial\xi}{\partial y}\,dx\,dy\Big|^2 \Bigg[\Big|\int_T (\mathbf{v}-\tilde{\mathcal{I}}\mathbf{v})DF^{-1}(2,:)\,dx\,dy\Big|^2 \\
& + \Big|\int_T (\alpha_{\ell,1}v_{\ell,1}+\alpha_{\ell,2}v_{\ell,2})\boldsymbol{n}_\ell DF^{-1}(2,:)\,dx\,dy\Big|^2\Bigg]\Bigg\} |\mathrm{b}_T(x,y)|^2_{1,T}/|\Delta|^2 \\
& + \sum_{T\subset\Omega_S:\mathcal{E}_T\cap\mathcal{E}_{\Gamma_I}\neq\emptyset} |(\alpha_{\ell,1}v_{\ell,1}+\alpha_{\ell,2}v_{\ell,2})\,n_{\ell,1}|^2_{1,T}\Bigg).
\end{aligned}
\tag{28}
$$

We observe that the constants $\alpha_{\ell,1}$ and $\alpha_{\ell,2}$ can be obtained by solving the nonsingular system (26) with $v_{\ell,i}|_T = (\hat{\delta}_{(0,0),\hat{T}_1}\hat{\delta}_{(1,0),\hat{T}_1}\hat{\beta}_{i,\hat{T}_1}) \circ F^{-1}_{\omega_\ell}(x,y)$.

More precisely, if we denote by $\beta_{\omega_\ell,j}$ to the continuous functions defined on ω_ℓ such that $\beta_{\omega_\ell,j}|_T = \beta_{T,j}$, $j=1,2$, by a simple calculation we can see that

$$
|\alpha_{\ell,j}| \leq \frac{C}{|\ell|}\max_{j=1,2}\Big|\int_\ell (\mathbf{v}-\tilde{\mathcal{I}}\mathbf{v})\cdot\boldsymbol{n}_\ell\ \beta_{\omega_\ell,j}\Big|
\tag{29}
$$

therefore,

$$
\begin{aligned}
& \int_T ((\alpha_{\ell,1}v_{\ell,1}+\alpha_{\ell,2}v_{\ell,2})\boldsymbol{n}_\ell DF^{-1}(1,:))^2 \\
\leq & C\int_T \Big((\alpha_{\ell,1}v_{\ell,1}+\alpha_{\ell,2}v_{\ell,2})n_{\ell,1}\frac{\partial\xi}{\partial x} + (\alpha_{\ell,1}v_{\ell,1}+\alpha_{\ell,2}v_{\ell,2})n_{\ell,2}\frac{\partial\xi}{\partial y}\Big)^2 \\
\leq & C\int_T \Big((\alpha^2_{\ell,1}v^2_{\ell,1}+\alpha^2_{\ell,2}v^2_{\ell,2})n^2_{\ell,1}\Big(\frac{\partial\xi}{\partial x}\Big)^2 + (\alpha^2_{\ell,1}v^2_{\ell,1}+\alpha^2_{\ell,2}v^2_{\ell,2})n^2_{\ell,2}\Big(\frac{\partial\xi}{\partial y}\Big)^2\Big).
\end{aligned}
$$

Using (14) and the inequality (29), we can affirm that

$$
\begin{aligned}
& C\int_T \Big((\alpha^2_{\ell,1}v^2_{\ell,1}+\alpha^2_{\ell,2}v^2_{\ell,2})n^2_{\ell,1}\Big(\frac{\partial\xi}{\partial x}\Big)^2 + (\alpha^2_{\ell,1}v^2_{\ell,1}+\alpha^2_{\ell,2}v^2_{\ell,2})n^2_{\ell,2}\Big(\frac{\partial\xi}{\partial y}\Big)^2\Big) \\
\leq & \frac{C}{h_T^2}\max_{i=1,2}|\alpha_{\ell,i}|^2\int_T (v^2_{\ell,1}+v^2_{\ell,2}) \\
\leq & \frac{C}{h_T^2|\ell|^2}\Big(\int_\ell |(\mathbf{v}-\tilde{\mathcal{I}}\mathbf{v})|\Big)^2\int_T (v^2_{\ell,1}+v^2_{\ell,2}).
\end{aligned}
$$

Using Cauchy-Schwarz and change of variables

$$
\begin{aligned}
& \frac{C}{h_T^2|\ell|^2}\Big(\int_\ell |(\mathbf{v}-\tilde{\mathcal{I}}\mathbf{v})|\Big)^2\int_T (v^2_{\ell,1}+v^2_{\ell,2}) \\
\leq & \frac{C|\ell|}{h_T^2|\ell|^2}\|\mathbf{v}-\tilde{\mathcal{I}}\mathbf{v}\|^2_{0,\ell}\int_T (v^2_{\ell,1}+v^2_{\ell,2}) \leq \frac{C}{h_T^2}\|\hat{\mathbf{v}}-\hat{\tilde{\mathcal{I}}}\mathbf{v}\|^2_{0,\hat{\ell}}\int_T (v^2_{\ell,1}+v^2_{\ell,2}).
\end{aligned}
$$

As $\|\hat{\mathbf{v}} - \hat{\tilde{\mathcal{I}}}\mathbf{v}(x)\|_{0,\hat{\ell}} \leq C|\hat{\ell}|^{\frac{1}{2}}\|\hat{\mathbf{v}}\|_{1,\hat{\omega}_{\hat{T}}}$, considering the definition of bubble functions, $v_{\ell,1}$ and $v_{\ell,2}$, and making a change of variables, we obtain

$$\begin{aligned}
&\frac{C}{h_T^2}\|\hat{\mathbf{v}} - \hat{\tilde{\mathcal{I}}}\mathbf{v}\|_{0,\hat{\ell}}^2 \int_T (v_{\ell,1}^2 + v_{\ell,2}^2)\\
\leq &\frac{C}{h_T^2}\|\hat{\mathbf{v}}\|_{1,\hat{\omega}_{\hat{T}}}^2 \int_T ((\hat{\delta}_{(0,0),\hat{T}_1}\hat{\delta}_{(1,0),\hat{T}_1}\hat{\beta}_{1,\hat{T}_1}) \circ F_{\omega_\ell}^{-1})^2 + ((\hat{\delta}_{(0,0),\hat{T}_1}\hat{\delta}_{(1,0),\hat{T}_1}\hat{\beta}_{2,\hat{T}_1}) \circ F_{\omega_\ell}^{-1})^2\\
\leq &\frac{C}{h_T^2}\|\hat{\mathbf{v}}\|_{1,\hat{\omega}_{\hat{T}}}^2 \int_{\hat{T}} (\hat{\delta}_{(0,0),\hat{T}_1}\hat{\delta}_{(1,0),\hat{T}_1})^2|J_F| \leq C\|\mathbf{v}\|_{1,\omega_T}^2
\end{aligned}$$

where in the last inequality we use that $\int_{\hat{T}} \hat{\delta}^{n_1}_{(0,0),\hat{T}}\hat{\delta}^{n_2}_{(1,0),\hat{T}} = \frac{n_1!n_2!2!}{(n_1+n_2+2)!}|\hat{T}|$ together with the bounded (14).

Therefore,

$$\begin{aligned}
&|\int_T (\alpha_{\ell,1}v_{\ell,1} + \alpha_{\ell,2}v_{\ell,2})\boldsymbol{n}_\ell DF^{-1}(1,:)\,|^2\\
\leq &|T|\,\|(\alpha_{\ell,1}v_{\ell,1} + \alpha_{\ell,2}v_{\ell,2})\boldsymbol{n}_\ell DF^{-1}(1,:)\|_{0,T}^2\\
\leq &Ch_T^2\|\mathbf{v}\|_{1,\omega_T}^2.
\end{aligned}$$

Moreover, by changing variables, using a classical inverse inequality and the previous observation we obtain

$$|(\alpha_{\ell,1}v_{\ell,1} + \alpha_{\ell,2}v_{\ell,2})n_{\ell,1}|_{1,T} \leq C\frac{1}{h_T}\|(\alpha_{\ell,1}v_{\ell,1} + \alpha_{\ell,2}v_{\ell,2})n_{\ell,1}\|_{0,T} \leq C\|\mathbf{v}\|_{1,\omega_T}.$$

Therefore, using these estimates in the expression (28) of the operator along with the fact that

$$\begin{aligned}
|\tilde{\mathcal{I}}_1\mathbf{v}(x,y)|_{1,T} &\leq C\|\mathbf{v}\|_{1,\omega_T},\\
|\int_T b_T\frac{\partial\eta}{\partial y}\,dx\,dy\,|^2 &\leq C\,h_T^2,\\
|\int_T b_T\frac{\partial\xi}{\partial y}\,dx\,dy\,|^2 &\leq C\,h_T^2,\\
|\int_T (\mathbf{v} - \tilde{\mathcal{I}}\mathbf{v})DF^{-1}(1,:)\,dx\,dy\,\Big| &\leq Ch_T^2\|\mathbf{v}\|_{1,\omega_T},\\
|\int_T (\mathbf{v} - \tilde{\mathcal{I}}\mathbf{v})DF^{-1}(2,:)\,dx\,dy\,\Big| &\leq Ch_T^2\|\mathbf{v}\|_{1,\omega_T},
\end{aligned}$$

as we proved earlier, we can conclude that

$$|\boldsymbol{\Pi}_h\mathbf{v}|_{1,\Omega_S} \leq C\|\mathbf{v}\|_1.$$

Finally, we want to estimate $\|\boldsymbol{\Pi}_h\mathbf{v}\|_{\mathbf{H}(\mathrm{div},\Omega_D)}$.

As $\|\boldsymbol{\Pi}_h\mathbf{v}\|_{\mathbf{H}(\mathrm{div},\Omega_D)} \leq \|\boldsymbol{\Pi}_h\mathbf{v}\|_{1,\Omega_D}$, with the same reasoning to the previous one for $|\boldsymbol{\Pi}_{h,j}\mathbf{v}|_{1,\Omega_S}^2$, we can conclude that

$$\|\boldsymbol{\Pi}_h\mathbf{v}\|_{1,\Omega_D} \leq C\|\mathbf{v}\|_1.$$

Then, we can say that the operator $\boldsymbol{\Pi}_h\mathbf{v}$ is bounded, that is, there is a positive constant C such that $\|\boldsymbol{\Pi}_h\mathbf{v}\|_{\mathbf{V}} \leq C\|\mathbf{v}\|_1$. □

The operator $\boldsymbol{\Pi}_h$ meets Lemmas 4.1 and 4.2 and therefore the inf-sup discrete condition is satisfied, that is, there is a positive constant β such that

$$\sup_{\mathbf{0}\neq\mathbf{v}_h\in\mathbf{V}_h}\frac{b(\mathbf{v}_h,q_h)}{||\mathbf{v}_h||_{\mathbf{V}}} \geq \beta||q_h||_Q, \forall\, q_h \in Q_h.$$

Since the bilinear form $\tilde{a}$ is coercive and continuous, b is continuous and satisfies the discrete inf-sup condition, using the abstract theory of mixed methods, we can enunciate the following results.

Theorem 4.1. *There exist a unique solution $(\mathbf{u}_h, p_h) \in \mathbf{V}_h \times Q_h$ of the problem (15).*

Theorem 4.2. *Let* $(\mathbf{u}, p) \in \mathbf{V} \times Q$ *be the solution of the weak formulation (5) of the coupled problem. Let* $(\mathbf{u}_h, p_h) \in \mathbf{V}_h \times Q_h$ *be the solution of the discrete problem (15). Then, there is a constant* C*, independent of the meshsize, such that:*

$$\|\mathbf{u}-\mathbf{u}_h\|_{\mathbf{V}} + \|p-p_h\|_Q \leq C\{\inf_{\mathbf{v}_h\in\mathbf{V}_h} \|\mathbf{u}-\mathbf{v}_h\|_{\mathbf{V}} + \inf_{q_h\in Q_h} \|p-q_h\|_Q\}.$$

Finally, considering that the classic error estimates of the Clèment interpolator can be extended to the case of domains with curved triangles (should be applied techniques similar to those used in, for example, Lemma 2 of [3]) and using the known results of Sobolev's space interpolation error (Theorem 1.4 of [27]) we can conclude the following result.

Corollary 4.1. *Let* $(\mathbf{u}, p) \in \mathbf{V} \times Q$ *be the solution of the weak formulation (5) of the coupled problem such that* $\mathbf{u} \in \mathbf{V}$ *and* $p \in Q$ *are smooth enough, that the norms on the right hand side of (30) are finite for some* $r_1, r_2 \in (0, 1]$*. Then, the discrete solution* $(\mathbf{u}_h, p_h)$ *of problem (15) satisfies the error estimation*

$$\|\mathbf{u}-\mathbf{u}_h\|_{\mathbf{V}} + \|p-p_h\|_Q \leq C\{h^{r_1}\|\mathbf{u}\|_{1+r_1,\Omega_S} + h^{r_2}\|\mathbf{u}\|_{1+r_2,\Omega_D} + h(|p|_{1,\Omega_S} + |p|_{1,\Omega_D})\}. \tag{30}$$

5. Numerical experiments

In this section we present some test cases to show the good performance of our method. We define the individual errors by,

$$e_0(p_S) = \|p_S - p_{S,h}\|_{0,\Omega_S} \qquad e_0(p_D) = \|p_D - p_{D,h}\|_{0,\Omega_D}$$
$$e_0(\mathbf{v}_S) = \|\mathbf{v}_S - \mathbf{v}_{S,h}\|_{0,\Omega_S} \qquad e_0(\mathbf{v}_D) = \|\mathbf{v}_D - \mathbf{v}_{D,h}\|_{0,\Omega_D}$$
$$e_0(\mathrm{div}\ \mathbf{v}_D) = \|\mathrm{div}(\mathbf{v}_D - \mathbf{v}_{D,h})\|_{0,\Omega_D} \qquad e_1(\mathbf{v}_S) = |\mathbf{v}_S - \mathbf{v}_{S,h}|_{1,\Omega_S}$$

and the rates of convergence are given by,

$$r_i(\Box) = \frac{log(\frac{e_i(\Box)}{e_i'(\Box)})}{log(\frac{h}{h'})} \qquad \Box \in \{\mathbf{v}_S, \mathbf{v}_D, \mathrm{div}\ \mathbf{v}_D, p_S, p_D\} \text{ and } i = 0, 1$$

where h and h' denote two consecutive mesh-sizes with errors e_i and e_i'. Using the previous

TABLE 1. Mesh-sizes, errors and rates of convergence (Example 1).

h	$e_0(\mathbf{v}_S)$	$r_0(\mathbf{v}_S)$	$e_0(\mathbf{v}_D)$	$r_0(\mathbf{v}_D)$	$e_0(p_S)$	$r_0(p_S)$	$e_0(p_D)$	$r_0(p_D)$
0.0308	0.0005	2.0243	0.0079	0.8383	0.0092	1.4152	0.0014	1.2806
0.0154	0.0001	2.0155	0.0041	0.9571	0.0033	1.4835	0.0006	1.3235
0.0077	0.0000	2.0058	0.0018	1.1371	0.0012	1.4983	0.0002	1.4158

TABLE 2. Mesh-sizes, errors and rates of convergence (Example 1).

h	$e_0(\mathrm{div}\ \mathbf{v}_D)$	$r_0(\mathrm{div}\ \mathbf{v}_D)$	$e_1(\mathbf{v}_S)$	$r_1(\mathbf{v}_S)$
0.0308	0.0101	0.8634	0.0922	1.0159
0.0154	0.0055	0.8869	0.0457	1.0114
0.0077	0.0028	0.9254	0.0228	1.0067

definition of r_i, we present for the first example, in Tables 1 and 2, the convergence history for a set of shape regular triangulations of the domain, in Tables 3 and 4, the corresponding for the second one and in Tables 5 and 6, the corresponding for the third example. For simplicity, in the first two examples, all the parameters such as K, α and μ are set to 1. We mention that, since is difficult to construct examples satisfying the entire coupled Stokes-Darcy problem (1)-(3) (in particular, the homogeneous interface conditions (3)), the numerical experiments could include nonhomogeneous terms for the

TABLE 3. Mesh-sizes, errors and rates of convergence (Example 2).

h	$e_0(\mathbf{v}_S)$	$r_0(\mathbf{v}_S)$	$e_0(\mathbf{v}_D)$	$r_0(\mathbf{v}_D)$	$e_0(p_S)$	$r_0(p_S)$	$e_0(p_D)$	$r_0(p_D)$
0.1884	0.0289	1.9518	0.0233	1.2349	0.2847	1.3193	0.0085	1.2560
0.0942	0.0072	2.0029	0.0097	1.2706	0.1060	1.4253	0.0031	1.4833
0.0471	0.0018	2.0103	0.0038	1.3562	0.0385	1.4628	0.0011	1.5378

TABLE 4. Mesh-sizes, errors and rates of convergence (Example 2).

h	$e_0(\text{div } \mathbf{v}_D)$	$r_0(\text{div } \mathbf{v}_D)$	$e_1(\mathbf{v}_S)$	$r_1(\mathbf{v}_S)$
0.1884	0.0258	0.8303	0.8102	0.9855
0.0942	0.0134	0.9451	0.4040	0.9990
0.0471	0.0068	0.9786	0.2012	1.0055

TABLE 5. Mesh-sizes, errors and rates of convergence (Example 3).

h	$e_0(\mathbf{v}_S)$	$r_0(\mathbf{v}_S)$	$e_0(\mathbf{v}_D)$	$r_0(\mathbf{v}_D)$	$e_0(p_S)$	$r_0(p_S)$	$e_0(p_D)$	$r_0(p_D)$
0.0313	0.0005	1.9831	0.0258	1.2013	0.0277	1.4229	0.0075	1.6198
0.0156	0.0001	1.9974	0.0105	1.2993	0.0100	1.4642	0.0025	1.5660
0.0078	0.0000	2.0037	0.0040	1.3787	0.0036	1.4823	0.0009	1.5296

TABLE 6. Mesh-sizes, errors and rates of convergence (Example 3).

h	$e_0(\text{div } \mathbf{v}_D)$	$r_0(\text{div } \mathbf{v}_D)$	$e_1(\mathbf{v}_S)$	$r_1(\mathbf{v}_S)$
0.0313	0.5056	0.9965	0.1378	1.0024
0.0156	0.2532	0.9974	0.0689	1.0013
0.0078	0.1268	0.9983	0.0344	1.0007

interface conditions and therefore is necessary to modify (only) the right-hand side in (5).

We also comment that, in practice, mass conservation and Neumann condition have to be imposed in a weak way. Indeed, when we assemble the system matrix we must add equations that ensures the normal continuity of the velocity and the boundary condition, i.e., $\int_\Gamma (\mathbf{v}_h^D \cdot \boldsymbol{n}_D + \mathbf{v}_h^S \cdot \boldsymbol{n}_S)\,\gamma = 0$ and $\int_{\Gamma_D} \mathbf{v}_h^D \cdot \boldsymbol{n}_D\,\gamma = 0, \quad \forall\, \gamma \in \{C^0(\Gamma) : \gamma|_\ell \in P_1(\ell)\}$.

5.1. First example: Curved boundary. We consider the regions $\Omega_S = \{(x,y) \in \mathbb{R}^2 : x \in (-1,1) \text{ and } 0 < y < \sqrt{1-x^2}\}$ and $\Omega_D = \{(x,y) \in \mathbb{R}^2 : x \in (-1,1) \text{ and } -\sqrt{1-x^2} < y < 0\}$. The interface results, $\Gamma_I = \{(x,y) \in \mathbb{R}^2 : x \in (-1,1) \text{ and } y = 0\}$ (see Figure 6). Note that both Γ_S and Γ_D are curved.

We select the right-hand terms $\mathbf{f}_S$, $g_S =:$ div $\mathbf{u}_S$, $\mathbf{f}_D$, g_D and the boundary conditions according to the analytical solution given by

$$\mathbf{u}_S(x,y) = \mathbf{u}_D(x,y) = \begin{pmatrix} -ye^{(x^2+y^2)}(1-(x^2+y^2)) \\ xe^{(x^2+y^2)}(1-(x^2+y^2)) \end{pmatrix}$$

$$p_S(x,y) = p_D(x,y) = cos(\pi(x^2+y^2)).$$

In this first example it is satisfied that $\mathbf{u}_D \cdot \boldsymbol{n_D} = 0$ in Γ_D, $\mathbf{u}_S = 0$ in Γ_S and $\mathbf{u}_D \cdot \boldsymbol{n}_D + \mathbf{u}_S \cdot \boldsymbol{n}_S = 0$ in Γ_I.

In Figures 7, 8, 9, 11, 12 and 13 we show the approximate and exact values of the velocities and in Figures 10 and 14 of the pressures. It is clear from these figures that the finite element spaces used provide very accurate approximations to the unknowns.

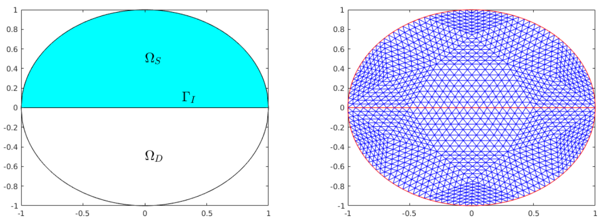

FIGURE 6. Full curved domain (Example 1).

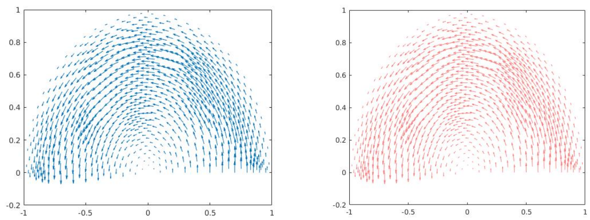

FIGURE 7. Vector charts $\mathbf{v}_S$ and $\mathbf{v}_{S,h}$ (Example 1).

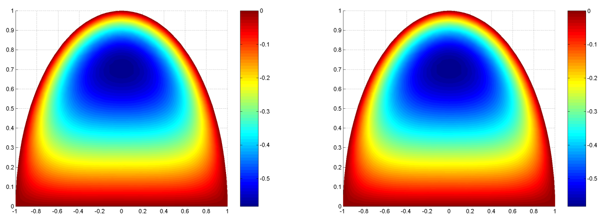

FIGURE 8. Contours of the first components of $\mathbf{v}_S$ and $\mathbf{v}_{S,h}$ (Example 1).

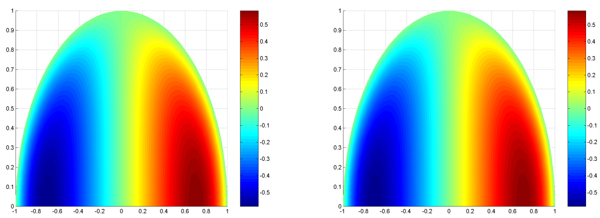

FIGURE 9. Contours of the second components of $\mathbf{v}_S$ and $\mathbf{v}_{S,h}$ (Example 1).

Tables 1 and 2 show that optimal rate of convergence can be also reached with our method.

5.2. Second Example: Curved interface. Let $\Omega_D = \{(x, y) \in \mathbb{R}^2 : x \in (-\frac{1}{2}, \frac{1}{2})$ and $0 < y < -x^2 + \frac{3}{4}\}$ and $\Omega_S = (-1, 1) \times (-1, 1) \setminus \Omega_D$ be a porous medium completely surrounded by a fluid (see Figure 15). The particularity of this example is that there is no Γ_D because

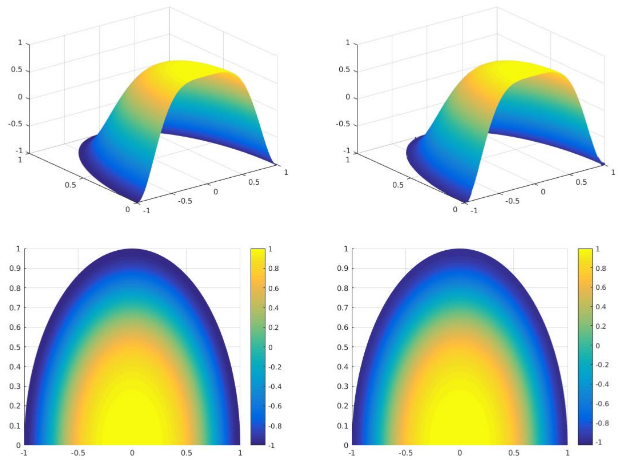

FIGURE 10. p_S and $p_{S,h}$ pressure figures (above) and pressure contours (bellow) (Example 1).

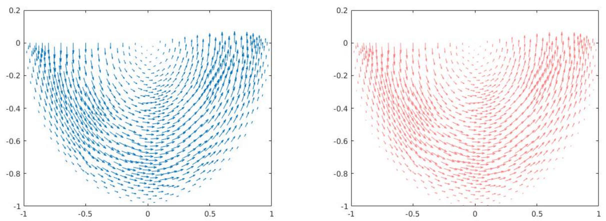

FIGURE 11. Vector charts $\mathbf{v}_D$ and $\mathbf{v}_{D,h}$ (Example 1).

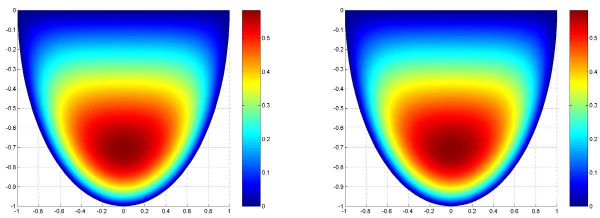

FIGURE 12. Contours of the first components of $\mathbf{v}_D$ and $\mathbf{v}_{D,h}$ (Example 1).

the boundary of Ω_D represent the interface, Γ_I. Note that one of the edges that make up the interface is being considered curved.

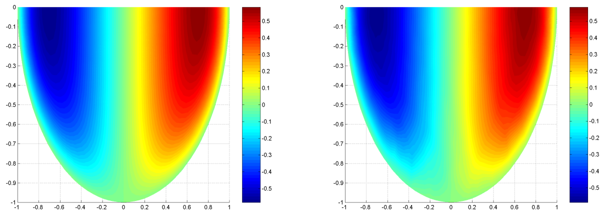

FIGURE 13. Contours of the second components of $\mathbf{v}_D$ and $\mathbf{v}_{D,h}$ (Example 1).

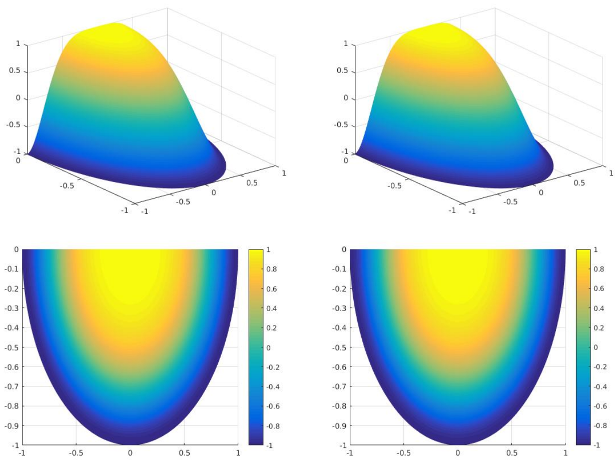

FIGURE 14. p_D and $p_{D,h}$ pressure figures (above) and pressure contours (Example 1).

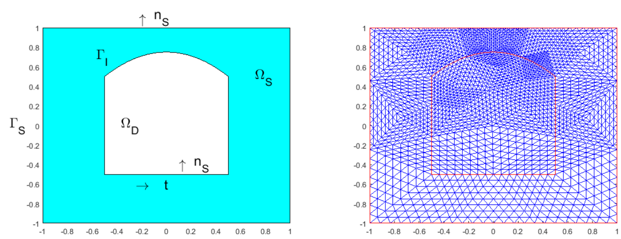

FIGURE 15. Full curved domain (Example 2).

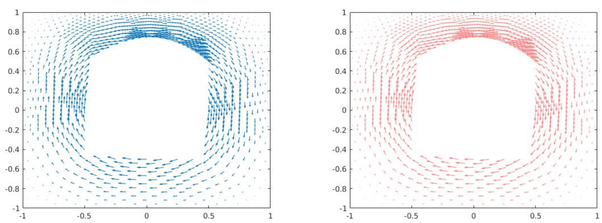

FIGURE 16. Vector chats $\mathbf{v}_S$ and $\mathbf{v}_{S,h}$ (Example 2).

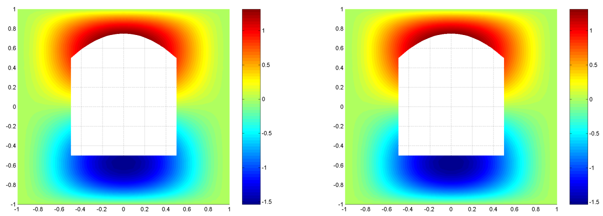

FIGURE 17. Contours of the First components of $\mathbf{v}_S$ and $\mathbf{v}_{S,h}$ (Example 2).

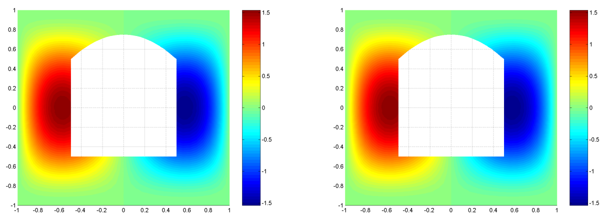

FIGURE 18. Contours of the second components of $\mathbf{v}_S$ and $\mathbf{v}_{S,h}$ (Example 2).

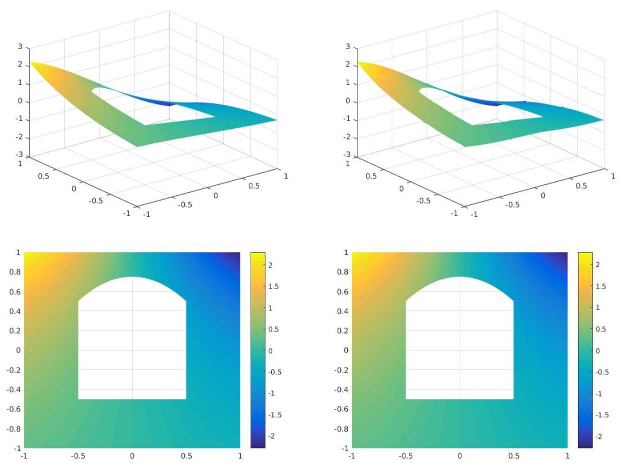

FIGURE 19. p_S and $p_{S,h}$, pressure figures (above) and pressure contours (bellow) (Example 2).

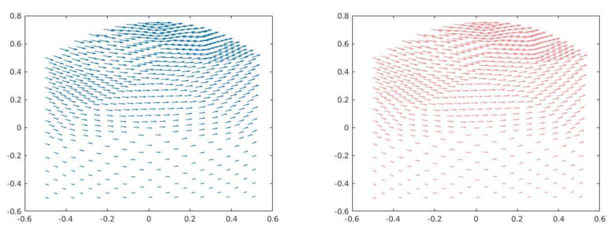

FIGURE 20. Vector charts $\mathbf{v}_D$ and $\mathbf{v}_{D,h}$ (Example 2).

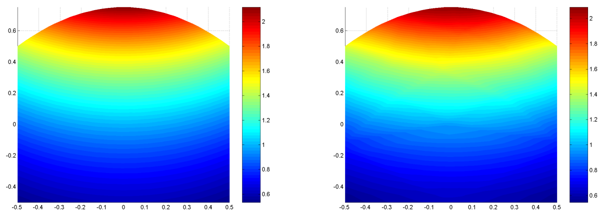

FIGURE 21. Contours of the first components of $\mathbf{v}_D$ and $\mathbf{v}_{D,h}$ (Example 2).

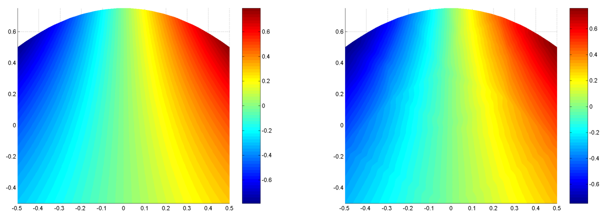

FIGURE 22. Second components of $\mathbf{v}_D$ and $\mathbf{v}_{D,h}$ (Example 2).

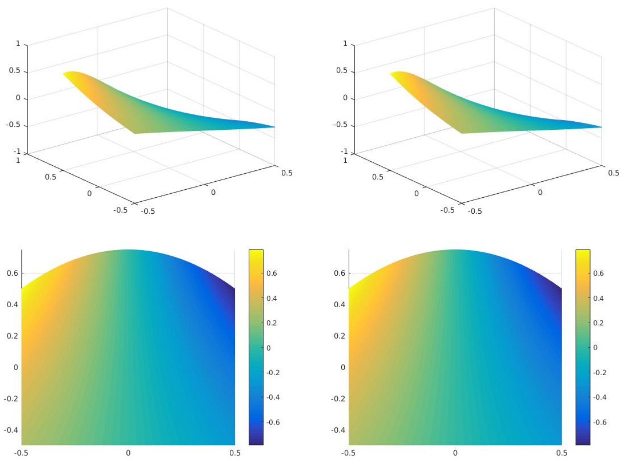

FIGURE 23. p_D and $p_{D,h}$, pressure figures (above) and pressure contours (bellow) (Example 2).

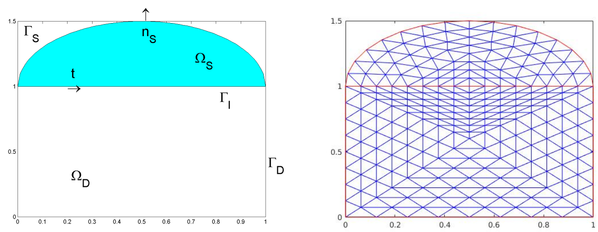

FIGURE 24. Full curved domain (Example 3).

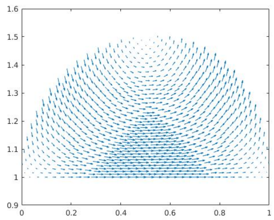

FIGURE 25. Vector chats $\mathbf{v}_S$ and $\mathbf{v}_{S,h}$ (Example 3).

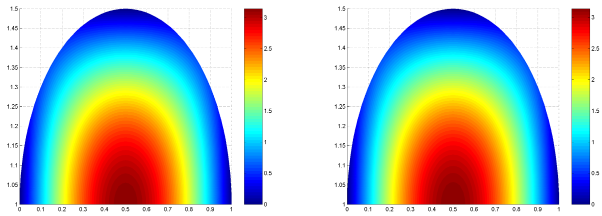

FIGURE 26. Contours of the first components of $\mathbf{v}_S$ and $\mathbf{v}_{S,h}$ (Example 3).

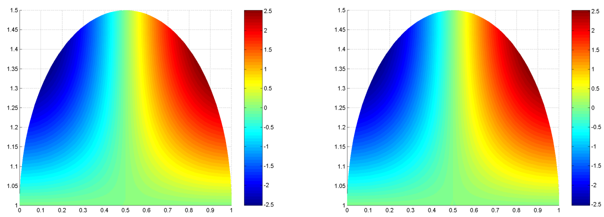

FIGURE 27. Contours of the second components of $\mathbf{v}_S$ and $\mathbf{v}_{S,h}$ (Example 3).

We set the appropriate forcing term $\mathbf{f}_S$ and the source g_D, such that the following solution to the Stokes-Darcy coupled problem, with $\mathbf{f}_D = \mathbf{0}$, is exact

$$\mathbf{u}_S(x,y) = \begin{pmatrix} -4(x^2-1)^2(y^2-1)y \\ 4(x^2-1)(y^2-1)^2x \end{pmatrix}$$

$$p_S(x,y) = -sin(x)e^y \qquad p_D(x,y) = -sin(x)e^y.$$

Figures 16 and 19 show, respectively, the approximate and exact velocities and the approximate and exact values of the pressure for the Stokes region, while Figures 20 and 23 display the corresponding figures for the Darcy region. Tables 3 and 4 show that optimal rate of convergence can be also reached with our method. Figures 17-18 and 21-22 show the first and the second component for the exact and approximate velocities for the Stokes region and the Darcy region.

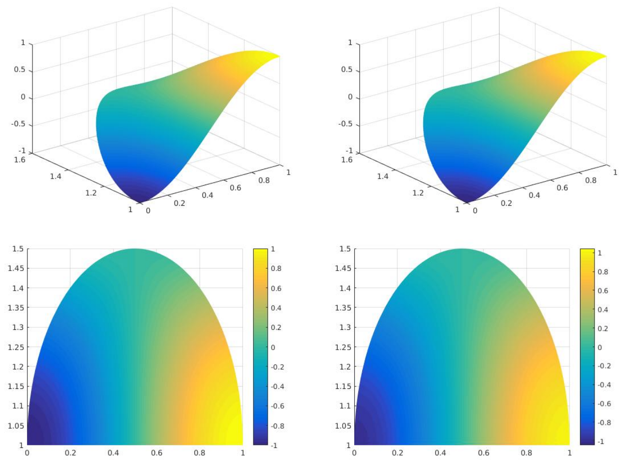

FIGURE 28. p_S and $p_{S,h}$, pressure figures (above) and pressure contours (bellow) (Example 3).

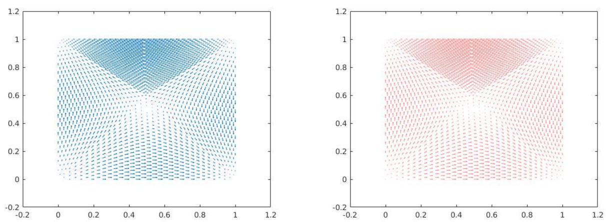

FIGURE 29. Vector charts $\mathbf{v}_D$ and $\mathbf{v}_{D,h}$ (Example 3).

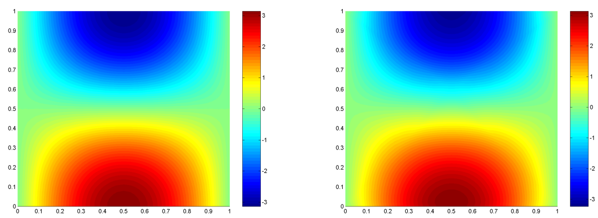

FIGURE 30. Contours of the first components of $\mathbf{v}_D$ and $\mathbf{v}_{D,h}$ (Example 3).

5.3. Third Example. The purpose of this third example, which matches with Example 1 in [19], is to confirm the good performance of our mixed finite element scheme in comparison with other stable elements. This example consist of a porous unit square, coupled with a semi-disk-shaped fluid domain, i.e., $\Omega_D = (0,1) \times (0,1)$ and $\Omega_S = \{(x,y) \in \mathbb{R}^2 : x \in (0,1) \text{ and } 1 < y < 1 + \sqrt{\frac{1}{4} - (x - \frac{1}{2})^2}\}$ (see Figure 24).

We set the appropriate forcing terms $\mathbf{f}_S$, $\mathbf{f}_D$ and the source g_D, such that the following solution to the Stokes-Darcy coupled problem is exact

$$\mathbf{u}_S(x,y) = \begin{pmatrix} -\pi sin(\pi x)cos(\pi y) \\ \pi cos(\pi x)sin(\pi y) \end{pmatrix} \qquad \mathbf{u}_D(x,y) = \begin{pmatrix} \pi sin(\pi x)cos(\pi y) \\ \pi cos(\pi x)sin(\pi y) \end{pmatrix}$$

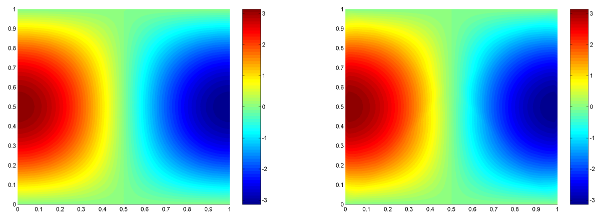

FIGURE 31. Contours of the second components of $\mathbf{v}_D$ and $\mathbf{v}_{D,h}$ (Example 3).

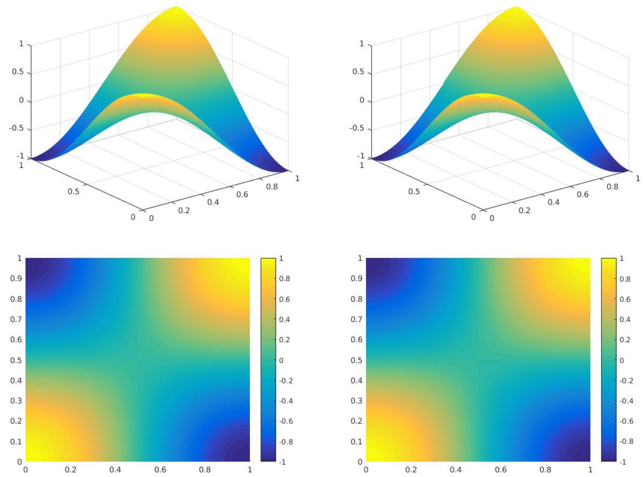

FIGURE 32. p_D and $p_{D,h}$, pressure figures (above) and pressure contours (bellow) (Example 3).

$$p_S(x, y) = cos(\pi x)cos(\pi y) \qquad p_D(x, y) = cos(\pi x)cos(\pi y).$$

Note that this solution satisfies $\mathbf{u}_D \cdot \boldsymbol{n}_D + \mathbf{u}_S \cdot \boldsymbol{n}_S = 0$ in Γ_I and the boundary condition $\mathbf{u}_D \cdot \boldsymbol{n_D} = 0$ in Γ_D. However the Dirichlet condition for the Stokes velocity in Γ_S is non-homogeneous.

Figures 25 and 28 show, respectively, the approximate and exact velocities and the approximate and exact values of the pressure for the Stokes region, while Figures 29 and 32 display the corresponding figures for the Darcy region. Tables 5 and 6 show that optimal rate of convergence can be also reached with our method. Figures 26-27 and 30-31 show the first and the second component for the exact and approximate velocities for the Stokes region and the Darcy region.

We also observe that, in the three examples under consideration, the rate of convergence provided by Corollary 4.1 is attained by all the unknowns.

To finish, in this example we study the effect of changing μ (the viscosity) and α in the variational formulation of the modified coupled problem (5). We run nine test with the different cases. The results are presented in Tables 7-9 .

We emphasize that the numerical results confirm the good performance of the mixed finite element scheme with MINI element for the Stokes-Darcy coupled problem. We end this paper by mentioning that, the ideas used here for numerical approximation of the coupled problem, could be successfully applied (with perhaps eventual technical difficulties) not only to another families of elements that are known to be stable for the Stokes problem if not also on 3D and it will be subject of future work.

Table 7. Rates of convergence for $\alpha = 1$.

μ	$r_0(\mathbf{v}_S)$	$r_0(\mathbf{v}_D)$	$r_0(p_S)$	$r_0(p_D)$	$r_0(\text{div } \mathbf{v}_D)$	$r_1(\mathbf{v}_S)$
1	1.9974	1.2993	1.4642	1.5660	0.9974	1.0013
0.1	1.9386	1.0624	1.4646	1.5740	0.9968	1.0015
0.01	2.0566	0.6926	1.5040	1.5624	0.9984	1.0079

Table 8. Rates of convergence for $\alpha = 0.1$.

μ	$r_0(\mathbf{v}_S)$	$r_0(\mathbf{v}_D)$	$r_0(p_S)$	$r_0(p_D)$	$r_0(\text{div } \mathbf{v}_D)$	$r_1(\mathbf{v}_S)$
1	1.9976	1.2993	1.4638	1.5659	0.9974	1.0013
0.1	1.9401	1.0624	1.4641	1.5740	0.9968	1.0015
0.01	2.0642	0.6925	1.5018	1.5624	0.9984	1.0081

Table 9. Rates of convergence for $\alpha = 0.01$.

μ	$r_0(\mathbf{v}_S)$	$r_0(\mathbf{v}_D)$	$r_0(p_S)$	$r_0(p_D)$	$r_0(\text{div } \mathbf{v}_D)$	$r_1(\mathbf{v}_S)$
1	1.9976	1.2993	1.4638	1.5659	0.9974	1.0013
0.1	1.9402	1.0624	1.4641	1.5740	0.9968	1.0015
0.01	2.0651	0.6925	1.5015	1.5624	0.9984	1.0081

References

[1] R. Araya, G. R. Barrenechea and A. Poza, An adaptive stabilized finite element method for the generalized Stokes problem, Journal of Computational and Applied Mathematics. 214 (2008) pp. 457-479.

[2] M. G. Armentano and J. Blasco, Stable and unstable cross-grid P_kQ_l mixed finite elements for the Stokes problem, Journal of Computational and Applied Mathematics. 234 (5), (2010) pp. 1404-1416.

[3] M. G. Armentano, C. Padra and M. Scheble, An hp finite element adaptive scheme to solve the Poisson problem on curved domains, Comput. Appl. Math., vol. 34 (2), pp. 705-727 (2015).

[4] M. G. Armentano and M. L. Stockdale, A unified mixed finite element approximations of the Stokes-Darcy coupled problem, Computers and Mathematics with Applications.

[5] D. N. Arnold, F. Brezzi and M. Fortin, A stable finite element for the Stokes equations, Calcolo 21 (1984) pp. 337-344.

[6] S. Badia and R. Codina, Stokes, Maxwell and Darcy: A single finite element approximation for three model problems, Applied Numerical Mathematics. 62 (2012) pp. 246-263.

[7] G. R. Barrenechea, L. P. Franca and F. Valentin, A Petrov-Galerkin enriched method: A mass conservative finite element method for the Darcy equation, Comput. Methods Appl. Mech. Engrg. 196 (2007) pp. 2449-2464.

[8] G. Beavers and D. Joseph, Boundary conditions at a naturally impermeable wall, Journal of Fluid Mechanics 30 (1967) pp. 197-207.

[9] C. Bernardi Optimal finite-element interpolation on curved domains SIAM J. Numer. Anal. 26 (5) (1989) pp. 1212-1240.

[10] P. B. Bochev and C. R. Dohrmann, A computational study of stabilized, low-order C0 finite element approximations of Darcy equations, Comput. Mech. 38 (2006) pp. 323-333.

[11] P. B. Bochev, C. R. Dohrmann, M. D. Gunzburger, Stabilization of low-order mixed finite elements for the Stokes equations, SIAM J. Numer. Anal. 44 (1) (2006) pp. 82-101.

[12] D. Boffi, *Minimal stabilizations of the P_{k+1}-P_k approximation of the stationary Stokes equations*, Mathematical Models & Methods in Applied Sciences 5 (2) (1995) pp. 213-224.

[13] D. Boffi, F. Brezzi, L. Demkowicz, R. G. Durán, R. Falk and M. Fortin, Mixed Finite Elements, Compatibility Conditions, and Applications, Lectures Notes in Mathematics, 1939, 2008.

[14] D. Boffi and L. Gastaldi, On the quadrilateral Q_2-P_1 element for the Stokes problem, International Journal for Numerical Methods in Fluids, 39 (4)(2002) pp. 1001-1011.

[15] D. Braess, Finite elements: Theory, fast solvers, and applications in solid mechanics, Cambridge University Press, 2007.
[16] F. Brezzi and R. Falk, Stability of higher-order Hood-Taylor methods, SIAM Journal on Numerical Analysis 28 (3) (1991) pp. 581-590.
[17] F. Brezzi and M. Fortin, Mixed and Hybrid Finite Element Methods, Springer, Berlin Heidelberg New York, 1991.
[18] F. Brezzi, M. Fortin and L. D. Marini, Mixed Finite Element Methods with continuous stresses, Math. Models Methods Appl. Sci. 3 (2) (1993) pp. 275287.
[19] J. Camao, G. N. Gatica, R. Oyarzúa, R. Ruiz-Baier and P. Venegas-Tapia New fully-mixed finite element methods for the Stokes-Darcy coupling, Computer Methods in Applied Mechanics and Engineering 295(1):362-395, 2015.
[20] P. G. Ciarlet, The Finite Element Method for Elliptic Problems, North Holland, Amsterdam, 1978.
[21] P. G. Ciarlet and J. L. Lions, Handbook of Numerical Analysis, Vol. 8. Gulf Professional Publishing, 1990.
[22] P. G. Ciarlet, P.A. Raviart, Interpolation theory over curved elements with applications to finite element methods, Comput. Methods Appl. Mech. Engrg., 1 pp. 217-249, 1972.
[23] M. Discacciati ans A. Quarteroni, NavierStokes/Darcy coupling: modeling, analysis, and numerical approximation, Rev. Math. Comput. 22 (2009) pp. 315-426.
[24] G. N. Gatica, S. Meddahi and R. Oyarzúa, *A conforming mixed finite-element method for the coupling of fluid flow with porous media flow*, IMA Journal of Numerical Analysis, 29 (2009) pp. 86-108.
[25] G. N. Gatica, R. Oyarzúa and F. J. Sayas, Analysis of fully-mixed finite element methods for the Stokes-Darcy coupled problem, Mathematics of Computation Vol. 80, Number 276 (2011) pp. 1911-1948.
[26] G. N. Gatica, R. Ruiz-Baier and G. Tierra, Giordano, A mixed finite element method for Darcy's equations with pressure dependent porosity, Math. Comp. 85 (297) (2016) pp. 133.
[27] V. Girault and P. A. Raviart, Finite Element Methods for Navier-Stokes Equations. Theory and Algorithms, Springer Series in Computational Mathematics, Vol. 5, Springer-Verlag, 1986.
[28] T. Karper, K. A. Mardal and R. Winther, Unified Finite Element Discretizations Of Coupled Darcy-Stokes Flow, Numerical Methods for Partial Differential Equations. 25 (2) (2009) pp. 311-326.
[29] W. J. Layton, F. Schieweck and I. Yotov, Coupling fluid flow with porous media flow, Siam J. Numer. Anal., 40 (6) (2003) pp. 2195-2218.
[30] N. S. Nicaise, B. Ahounou and W. Houedanou, Residual-based a posteriori error estimates for a nonconforming finite element discretization of the Stokes-Darcy coupled problem: isotropic discretization, Afr. Mat. 27, No. 3-4 (2016) pp. 701729.
[31] P. A. Raviart and J. M. Thomas, A mixed finite element method for second order elliptic problems, Mathematical Aspects of the Finite Element Method, (I. Galligani, E.Magenes,eds.), Lectures Notes in Math. 606, Springer Verlag, 1977.
[32] H. Rui and R. Zhang, A unified stabilized mixed finite element method for coupling Stokes and Darcy flows, Comput. Methods Appl. Mech. Eng. 198 (2009) pp. 2692-2699.
[33] R. Scott, Interpolated boundary conditions in the finite element method, SIAM J. Numer. Anal., 12 pp. 404-427 (1975).
[34] P. Song, C. Wang and I. Yotov, Domain Decomposition for Stokes-Darcy Flows with Curved Interfaces Procedia Computer Science 18 (2013) pp. 1077-1086.
[35] R. Verfürth, A Posteriori Error Estimation Techniques for Finite Element Methods, Numerical Mathematics and Scientific Computation, Oxford University Press, Oxford, (2013).
[36] S. Weiber, Residual error estimate for BEM-based FEM on polygonal meshes, Numerische Mathematik 118 (4) (2011) pp. 765-788.
[37] M. Zlamal, Curved elements in the finite element methods I, SIAM J. Numer. Anal. 10(1), pp. 229-240,(1973).

Departamento de Matemática, Facultad de Ciencias Exactas y Naturales, Universidad de Buenos Aires, 1428, Buenos Aires, Argentina.

IMAS, Conicet, 1428, Buenos Aires, Argentina.
E-mail: garmenta@dm.uba.ar

Departamento de Matemática, Facultad de Ciencias Exactas y Naturales, Universidad de Buenos Aires, 1428, Buenos Aires, Argentina.
E-mail: mlstockdale@dm.uba.ar